Chapter 10
Infrared, Raman, and Fluorescence Spectroscopies: Methodologies and Applications

Diego L. García-González, Vincent Baeten, Juan A. Fernández Pierna, and Noelia Tena

Contents

D.L. García-González (✉) • N. Tena
Instituto de la Grasa (CSIC), Avda. Padre García Tejero 4, 41012 Sevilla, Spain
e-mail: dluisg@cica.es; noelia.tena@ig.csis.es

V. Baeten • J.A. Fernández Pierna
Walloon Agricultural Research Centre, Chaussée de Namur 24, 5030 Gembloux, Belgium
e-mail: baeten@cra.wallonie.be; fernandez@cra.wallonie.be

R. Aparicio and J. Harwood (eds.), *Handbook of Olive Oil: Analysis and Properties*,
DOI 10.1007/978-1-4614-7777-8_10,

Abbreviations

ANN	Artificial neural network
ATR	Attenuated total reflectance
CCD	Coupled charge device
CV	Coefficient of variation
EEFS	Excitation-emission fluorescence spectroscopy
FF	Front face
FT	Fourier transform
IRE	Internal reflection element
MIR	Mid-infrared
MLR	Multiple linear regression
MSE	Multiple standard error
NIR	Near-infrared
NMR	Nuclear magnetic resonance
OPL	Optical path length
PCA	Principal component analysis
PCR	Principal component regression
PLSR	Partial least-squares regression
PLS	Partial least squares
PLSDA	Partial least-squares discriminant analysis
RA	Right angle
RHM	Resampling by half-means
SD	Standard deviation
SFS	Synchronous fluorescence spectroscopy
SHV	Smallest half-volume
SLDA	Stepwise linear discriminant analysis
SMD	Squared Mahalanobis distances
SMLR	Stepwise multiple linear regression
SVM	Support vector machines

10.1 Introduction

Spectroscopic techniques have emerged in food analysis as rapid and very useful tools for determining a great variety of chemical parameters. They provide elegant solutions to face analytical challenges. In spite of the intense research on

spectroscopic techniques during the twentieth century, the application of such techniques has been delayed due to the spread of chromatography, which allows an easy quantitative interpretation of results, and the lack of suitable sample presentation techniques, chemometric tools to calibrate and standardize instruments, intuitive chemometric tools, and standardized protocols for spectroscopy. However, the necessity of reducing the analytical time and cost, the high number of parameters and properties to be simultaneously controlled at the different steps of the food and feed chains, and the increasing demand for online techniques, as well as the relative limit of traditional techniques to solve some analytical questions faced by the control laboratories and industries, have rekindled interest in spectroscopy techniques. Furthermore, instrumental improvements such as the introduction of interferometry methodology and the diode array detector, the availability of new sample-handling accessories, the miniaturization of instruments, the computer facilities, and the existence of software specially designed to extract and to use the information contained in spectra have contributed to the development of near-infrared (NIR), mid-infrared (MIR), Raman, and fluorescence spectroscopies. These significant improvements have led to less complicated and expensive instruments that could be used on a regular basis at any laboratory without requiring any special skills or training.

In the field of fats and oils quantitative applications are relatively recent compared to qualitative methodologies. These quantitative procedures have benefited from new ways of calibration (e.g., signal-transduction calibration), adapted accessories for sample presentation (e.g., ATR, IR cards, and mesh cells), and adopted new procedures of spectra interpretation (e.g., 2D correlation spectroscopy). The great variety of optical materials and sampling approaches makes the spectroscopic techniques much more versatile than other methodologies, which explains the growing interest in developing quantitative applications. Although there are only few standard methodologies for olive oil analysis based on spectroscopy (e.g., determination of dienes and trienes by ultraviolet spectroscopy, COI/T.20/Doc. No 19/Rev. 2), a spectroscopic technique such as Fourier transform infrared spectroscopy (FT-IR) can be applied to determine the unsaturation degree, oxidation state, moisture content, *trans* double bonds, free fatty acids, and the presence of impurities or other edible oils, among many others. Such applications require more research to improve calibration performance without losing the advantageous feature of being rapid methods. Such research might deliver methodologies that could be eligible as standard methods in the future to alleviate complex olive oil analysis.

In this chapter, the second and third sections briefly present the theory and instrumentation currently used in IR, Raman, and fluorescence spectroscopies for the analysis of oils. The fourth section describes data acquisition, and the fifth section is dedicated to interpretation of oil spectra. The assignment of the most noteworthy bands and the correlation between absorption (or scattering) intensities and chemical indices are discussed. Part of this chapter (the sixth section) is devoted to the data treatment of IR and Raman spectra. In this section, a mathematical model construction in quantitative and qualitative analyses is presented. Finally, the results obtained in the determination of chemical values and indices are surveyed in the seventh section.

10.2 Theory

The importance of spectroscopy becomes apparent from a reading of the classic text published by Herzberg (1945). However, it was not until recently that dramatic progress was made with the advent of IR lasers (e.g., IR circular dichroism) and inteferometric methods, the introduction of high-power and pulsed lasers (e.g., hyper-Raman and coherent anti-Stokes-Raman scattering), or attenuated total reflection (ATR) spectroscopy, among others. Thus, spectroscopy is not a static field; it is a quite dynamic and innovative area. Regarding vibrational spectroscopy, the basic theory has been described in ten or so classic books on spectroscopy, some of which are compilations of data while others are comprehensive texts (Wilson et al. 1955; Williams and Norris 2001; Li-Chan et al. 2010a, b). Most practical books usually emphasize the correlation between molecular structural features and frequencies (Socrates 1994), while textbooks are devoted to explaining the theory of vibrational spectroscopy (Williams and Norris 2001; Diem 1993). Concerning fluorescence spectroscopy, modern manuals explaining the fundamentals and applications illustrate the increasing interest in this technique for developing applications beyond basic research (Valeur 2002).

The following section will briefly describe those theoretical aspects of IR, Raman, and fluorescence spectroscopies that are basic for understanding spectroscopic analyses.

10.2.1 Infrared Spectroscopy

Infrared spectroscopy is a technique in which the interaction of electromagnetic radiation with a sample is studied to obtain both qualitative and quantitative chemical information. The IR region lies between the red end of the visible spectrum and the microwave region. It comprises wavelengths (λ) between 800 and 2.5×10^5 nm. The IR region of the electromagnetic spectrum is subdivided into NIR (λ=0.8–2.5 μm), MIR (λ=2.5–25 μm), and far-IR (λ=50–1,000 μm). These distinctions are based on the nature of the absorptions giving rise to the corresponding spectra, as well as differences in instrumental design and experimental approach. All are parts of vibrational spectroscopy and arise from transitions between vibrational energy levels (Banwell 1994).

The simplest approach to explaining the phenomenon occurring in vibrational spectroscopy is to consider the bond between two atoms of masses m_1 and m_2 as behaving as a tiny spring of "strength," or force constant k ($N^* m^{-1}$). The system will vibrate at some natural resonance frequency ν (s^{-1}) given by Hooke's law:

$$\nu = \frac{1}{2\pi}\sqrt{\frac{\kappa}{\mu}},$$

where μ is the "reduced mass" $[m_1m_2/(m_1+m_2)]$. This approach is used to explain the observed difference in absorption frequencies between different functional groups on the basis of different force constants or reduced masses.

However, the quantum theory needs to be considered here. The energy E (J) of a photon of wavelength λ (m) is

$$E = h\nu = h\frac{c}{\lambda}.$$

In this equation h (Js) is Planck's constant and c (ms^{-1}) is the velocity of light.

Hooke's law for a simple harmonic oscillator model predicts a potential energy curve as a parabolic function of the interatomic distance. The potential energy is minimized at the equilibrium nuclear distance. Increasing interatomic distance leads to increased potential energy in a continuous manner. In a quantum mechanical approach (corpuscular theory), however, only certain energy levels are permitted. These energy levels are given by

$$E(n) = \left(n + \frac{1}{2}\right)h\nu,$$

where $n = 0,1,2\ldots$ is the vibrational quantum number. Transition between energy levels can only occur in discrete steps when sufficient energy E is provided, i.e.,

$$\Delta E = h\nu.$$

Transitions occur when $n \geq \pm 1$. The molecule will absorb the energy of the photon if it precisely matches the energy that is required for the transition between energy levels and when there is a change in the dipole moment associated with the vibration. The transitions in which $n = \pm 1$ are called fundamental vibrations and they are observed in MIR spectroscopy. The energy required to stimulate these transitions occurs at wavelengths between 2,500 and 25,000 nm (4,000–400 cm^{-1}).

In fact, vibrating bonds are anharmonic oscillators. When the interatomic distance becomes very small, atomic repulsion causes the potential energy to rise dramatically. As the interatomic distance increases, the bond will initially stretch and eventually break. This anharmonic behavior can be incorporated into the Schrödinger equation and leads to a new expression for permitted energy levels:

$$E(n) = \left(n + \frac{1}{2}\right)h\nu - \left(n + \frac{1}{2}\right)^2 x_e h\nu,$$

where x_e is a small and positive anharmonicity constant.

As a result of anharmonicity, energy levels become closer as n increases and transitions of the type $n = \pm 2$, $n = \pm 3$, or overtones are allowed. In addition, a combination band is produced when the photon excites simultaneously the vibration of two or more interatomic bonds that are sufficiently close to influence their respective vibrations. Combinations and overtones are seen at higher energy (lower wavelength) and occur in the NIR region (800–2,500 nm; 10,000–4,000 cm^{-1}). These bands

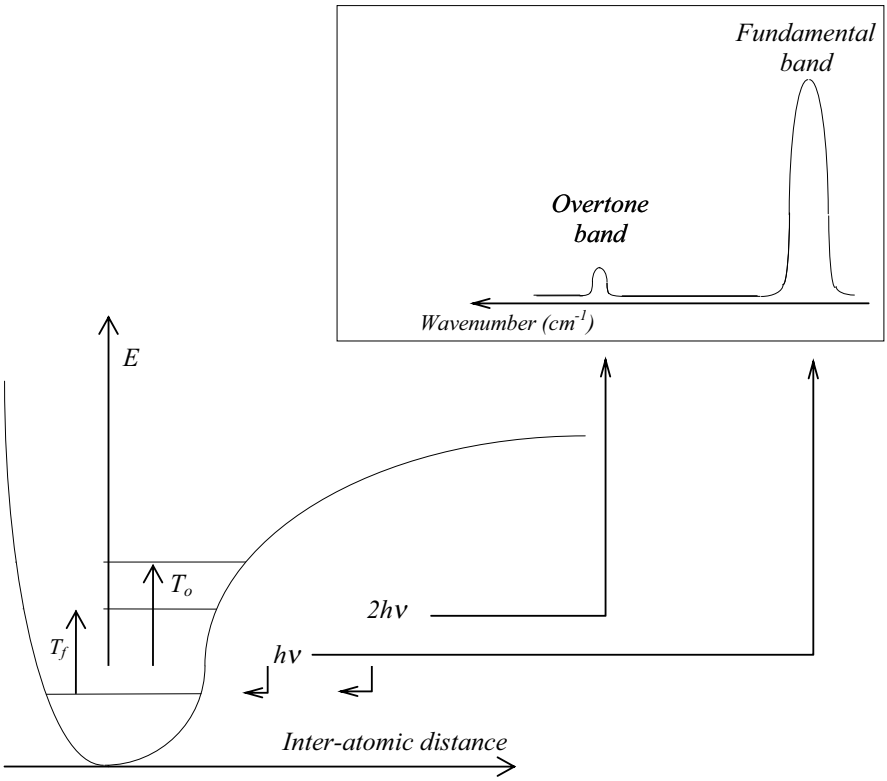

Fig. 10.1 Anharmonic oscillator and associated energetic transitions. Legend: E potential energy, T_f fundamental transition, T_o overtone transition

have lower intensity than fundamental bands. Figure 10.1 illustrates the anharmonic oscillator and the different associated energetic transitions (Barrow 1973; Williams and Norris 2001; Skoog et al. 1992).

10.2.2 Raman Spectroscopy

Raman spectroscopy involves a scattering process. When the electric field E interacts with a molecule, it exerts the same force on all electrons in the molecule and tends to displace them from their original position around the positively charged nuclei. The displacements result in an induced dipole moment π in the molecule that is proportional to the electric field:

$$\pi = \alpha E,$$

where α is the electric polarizability. Since π depends on α as well as E, the properties of the molecule can change π. In this context, α varies with time as a consequence of the vibrations of the molecule since the ease with which electrons may be displaced by the electric field depends on how tightly they are bound to the nuclei, which in turn depends on the interatomic distance.

When the electric field interacts with a vibrating molecule, the induced dipole moment has three components contributing to its time dependence. The first is a component vibrating with the frequency of the incident light. According to classical electromagnetic theory, an oscillating dipole radiates energy in the form of scattered light. Thus, the first component, light of the incident frequency (ν_{Ray}), will be scattered. This is the phenomenon of Rayleigh scattering. The second component is the one vibrating at a frequency that is the sum of the frequencies of the incident light and the molecular vibration. The scattered light arising from this second component is known as anti-Stokes Raman scattering ($\nu_{R(aSt)}$). The third component is the vibration at a frequency given by that of the incident light minus the molecular vibrations. This is called Stokes scattering ($\nu_{R(St)}$) (Grasseli and Bulkin 1991; Diem 1993; Schrader 1996).

Figure 10.2 shows an energy diagram of the Raman scattering effect and illustrates a schematic and simplified Raman spectrum. To simplify the presentation, only two electronic states (the ground and the first excited) and three vibrational states of each of them are shown. The intensity of the anti-Stokes Raman scattering bands of frequency < *R(aSt)* is lower than the intensity of Stokes Raman scattering bands of frequency < *R(St)* in view of the difference in population of the ground excited electronic states in a set of molecules at room temperature (Baranska et al. 1987). The Raman spectra studied and presented later on in this chapter concern only Raman Stokes scattering bands.

10.2.3 Fluorescence Spectroscopy

Fluorescence spectroscopy is a type of electromagnetic spectroscopy in which the fluorophore groups included in the samples are excited using a beam of light. Usually ultraviolet light is used and the emission of light of a lower energy is observed; typically, but not necessarily, the emission is in the visible range of the electromagnetic spectrum. In particular, conventional fluorescence spectroscopy provides an emission spectrum for a fixed excitation wavelength or an excitation spectrum for a fixed emission wavelength. The emission spectra are obtained by recording the signal of an emission monochromator at different wavelengths (λ_{em}) for a constant excitation wavelength (λ_{ex}), usually at a wavelength of high absorption. On the other hand, the excitation spectra are obtained by recording the signal from the excitation monochromator at different wavelengths (λ_{ex}), maintaining a constant emission wavelength (λ_{em}). The spectra provide information for both qualitative and quantitative analyses about fluorophore groups present in the sample. However, the applications of fluorescence spectroscopy in the characterization of edible oils are scarce because the fluorescence

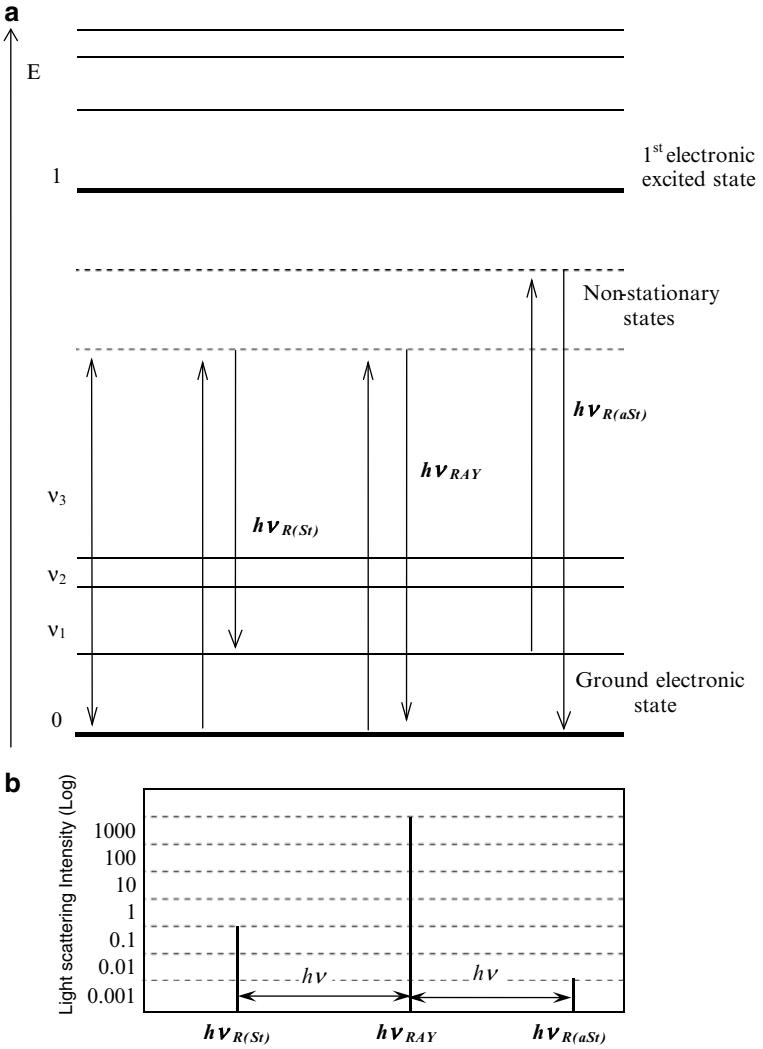

Fig. 10.2 (**a**) Raman scattering effect occurring during illumination of sample with monochromatic light. (**b**) Part of resulting Raman spectrum. Legend: *E* electronic state, *I* light-scattering intensity (log scale), ν_{Ray} frequency of Rayleigh line, $\nu_{R(aSt)}$ frequency of anti-Stokes Raman line, $\nu_{R(St)}$ frequency of Stokes Raman line (Adapted from Baranska et al. 1987)

characteristics of fluorophores are affected by the matrix. Although molecular fluorescence spectroscopy is a highly sensitive technique, a severe overlap of excitation and emission makes the spectra difficult to interpret (Patra and Mishra 2002). The fluorescence spectra can also be affected by the attenuation of the absorption intensity due to the absorption of the excitation wavelength (primary inner effect) and the emission wavelength (secondary inner effect) (Sikorska et al. 2004). These phenomena are more evident when working with right angle (RA) instruments (Lakowicz 1999). In RA

instruments, the collection of the fluorescence beam is collected at a right angle to the incident light. In other words, the emission is measured at 90° in relation to the excitation beam. In contrast, in modern front face (FF) instruments, the fluorescence beam is collected at an approximately 22–30° angle relative to the incident beam. This geometry minimizes the inner filter effects compared to RA instruments.

10.2.4 Band Position and Intensity

In vibrational spectroscopy, the probability of excitation for a particular vibration is determined by the so-called selection rules, which can be derived from the application of group theory to atomic vibrations in the molecules belonging to different classes of symmetry. Some factors tend to modify the band positions (i.e., vibration frequencies). The most important factors are the interatomic distances, the spatial arrangement groups, the Fermi resonance, the physical state of the sample, the polarity of the environment, the formation of hydrogen bonds, and the inductive, mesomeric, and field effects of neighboring groups. In this way, the difference in the force constant, for example, explain that the stretching frequency of double bonds is higher than those of single bonds (Baranska et al. 1987; Grasseli and Bulkin 1991; Diem 1993).

Infrared and Raman spectroscopy involve vibrational energy levels of the sample molecules that are related primarily to stretching or bending deformations of the molecular bonds. However, two main differences should be underlined between IR and Raman spectra. First, IR peaks tend to be broad and it is difficult to find a peak that is completely free of the influence of adjacent peaks or external parameters. On the other hand, a Raman spectrum tends to be composed of a series of isolated bands, and water and CO_2 have weak Raman scattering properties and, consequently, produce less interference in Raman scattering spectroscopy. Another difference is that polar groups (such as C=O and O-H) have strong IR absorption bands, whereas nonpolar groups (such as C=C and C-C) show intense Raman scattering bands. These two branches of vibrational spectroscopy in fact yield complementary information about molecular vibration, each one contributing to a spectral fingerprint of the molecules (Li-Chan 1994).

From a chemical point of view, Raman scattering arises from the change in polarizability or shape of the electron distribution in the molecule as it vibrates; in contrast, IR absorption requires a change in the intrinsic dipole moment with the molecular vibration (Grasseli and Bulkin 1991). More accurately, the Raman band intensity is proportional to the expression

$$\left(\partial\alpha / \partial Q\right)^2,$$

where α is the polarizability and Q the normal coordinate of the group of atoms of interest. The IR band intensity is proportional to the expression

$$\left(\partial\pi / \partial Q\right)^2,$$

where π is the induced dipole moment of the molecule. Thus, it might be expected that the same molecule may give IR and Raman bands with differing intensities and band shapes (Baranska et al. 1987).

Concerning fluorescence spectroscopy, to study the band position and intensity it is necessary to consider the following issues:

1. The excitation wavelength used to obtain the emissions spectra should be strongly absorbed by the fluorescent compounds; therefore it is recommended to obtain the full absorption spectrum of the sample and then select the most appropriate wavelength based on the maximum absorption intensities. It is important to use an excitation wavelength that is strongly absorbed because the emission fluorescence intensity is proportional to the absorption intensity.
2. Not all of the emission spectrum obtained with the selected excitation wavelength corresponds to the fluorescent compounds present in the sample. According to Stokes's law of fluorescence states, the wavelength of fluorescence radiation is greater than the exciting radiation. Consequently, the emission wavelengths should be at least five or ten units larger than the excitation wavelength. For example, for an excitation wavelength (λ_{ex}) at 350 nm, the bands that appear in the emission spectrum at wavelengths below 360 nm do not correspond to fluorescent compounds.
3. Other additional considerations that could lead to error are associated with overtones. Thus, it is important to note that the overtone area is located at twice the wavelength of excitation in the emission spectrum. In the interpretation of the spectra it is also convenient to omit the region of the spectrum that is located too far from the excitation wavelength (Fig. 10.3).
4. Primary and secondary inner filter effects are other considerations that should be taken into account in the traditional RA techniques (Lakowicz 1999). The inner filter effects imply the attenuation of the emission intensity due to the absorption of the incident excitation light and emitted light (Sikorska et al. 2004). These effects are avoided by working with diluted samples – in the case of oils, 1 % is enough. This solution also prevents saturation in the spectrum. Nevertheless, the spectra obtained from diluted samples are not always comparable to those obtained with original undiluted samples. This difference in the spectra is due to the original environment of the samples, which dramatically changes when they are diluted, and this could have a significant effect given that fluorescence properties are extremely sensitive to matrix changes (Strasburg and Ludescher 1995). To overcome this problem and examine native samples directly, the FF technique is more appropriate.

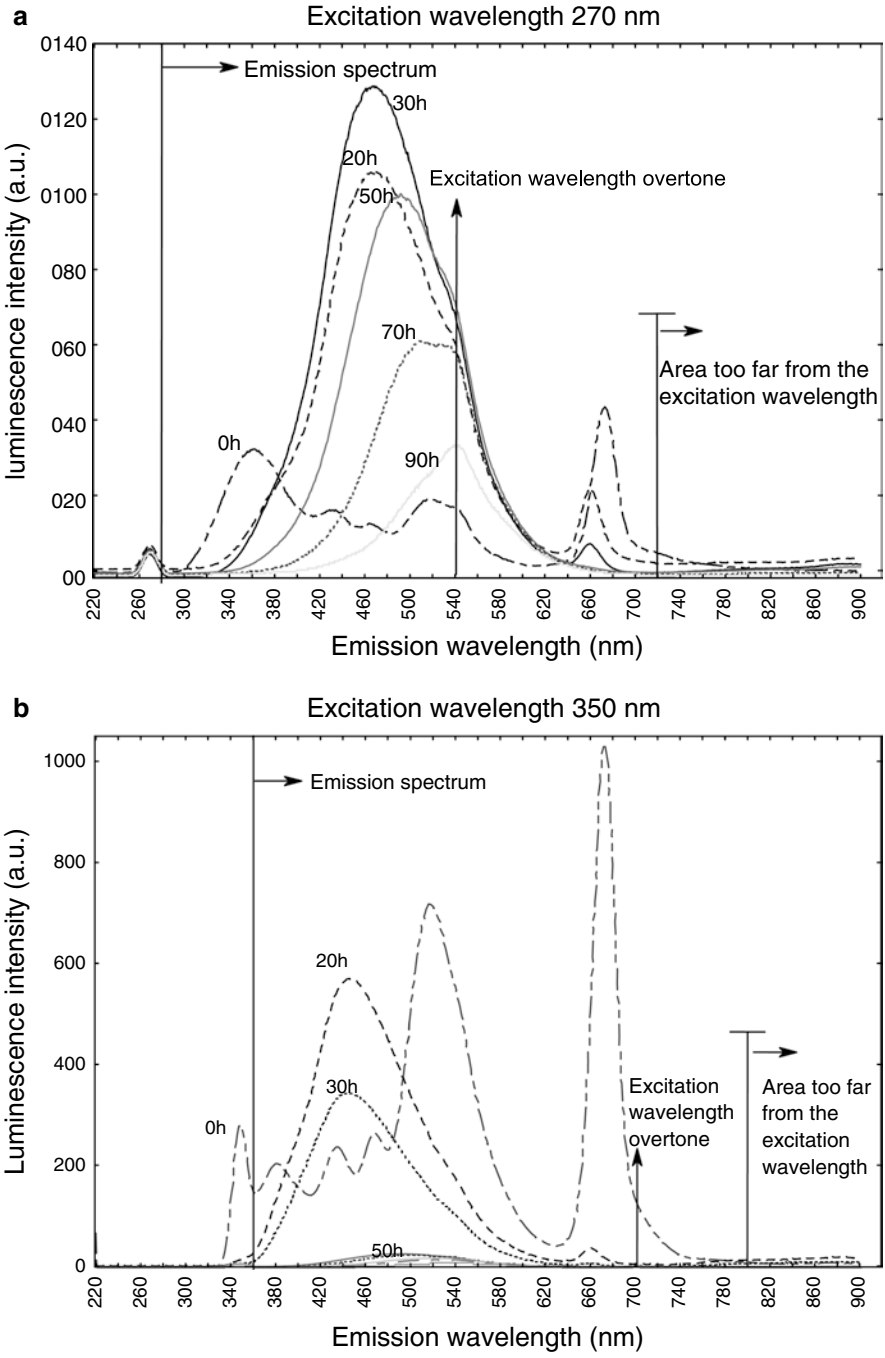

Fig. 10.3 Fluorescence emission spectra of virgin olive oils differing in their thermoxidation times (hours) collected under two different excitation wavelength: $\lambda_{exc} = 270$ nm (**a**) and $\lambda_{exc} = 350$ nm (**b**)

10.3 Instrumentation

Two of the main reasons for the development of new applications of spectroscopic techniques are the simplicity of the equipment and the sample presentation. Samples can be examined in their gaseous, liquid, or solid states. Enormous progress has been made, particularly over the two last decades, on the instrumental front (Diem 1993; Sharma and Schulman 1999; Li-Chan et al. 2010a).

Spectrometers can be classified according to the radiation source used, either thermal or nonthermal. Thermal sources (e.g., quartz-halogen or tungsten-halogen lamps) consist of a radiant filament that produces thermal radiation covering a narrow or wide range of frequencies in the vibrational spectral range. Nonthermal sources (e.g., light-emitting diodes, laser diodes, or lasers) emit narrower bands of radiation than those emitted by thermal sources. Another classification of spectrometers is based on the wavelength selection strategy: discrete or continuous wavelength selection. Discrete wavelength instruments, using filters or light-emitting diodes, make it possible to collect the absorbance at specific wavelengths and are not widely used. Continuous-spectrum instruments are based on grating monochromator, acousto-optical tunable filter, photodiode array, Fourier transform (FT) interferometer technologies, or microelectromechanical systems (MEMS) (Osborne et al. 1993; Williams and Norris 2001; Blanco and Villaroya 2002).

10.3.1 Near-Infrared (NIR) Spectroscopy

NIR instruments have been widely used for nondestructive rapid analysis in several important industries since the early 1970s. In the animal feed, grain, chemical, pharmaceutical, and food industries, NIR spectroscopy is used in offline, online, and inline modes. Several optical approaches have been used in NIR instruments, including filters, holographic gratings, acousto-optically tunable filters, light-emitting diodes, and the internal and external fitting of optic fibers (Scotter 1997; Osborne et al. 1993; Williams and Norris 2001).

Four configurations of spectral collection exist: transmission, transflection, diffuse reflection, and interactance. This has been addressed in detail by Wilson and Goodfellow (1994). In oil analysis, transmission and transflection modes are traditionally used and correspond to specific sample-handling designs. An important feature of NIR spectroscopy is that the shorter NIR wavelengths can penetrate deeply into the sample; thus, it is possible to obtain spectral data from a thick sample (i.e., 1–5 mm). In addition, classic crystal and quartz materials are free of absorbance in the NIR region.

A transmission cell is used to obtain spectra of liquids and slurries. To make a transmission measurement, the sample accessory is placed between the source and

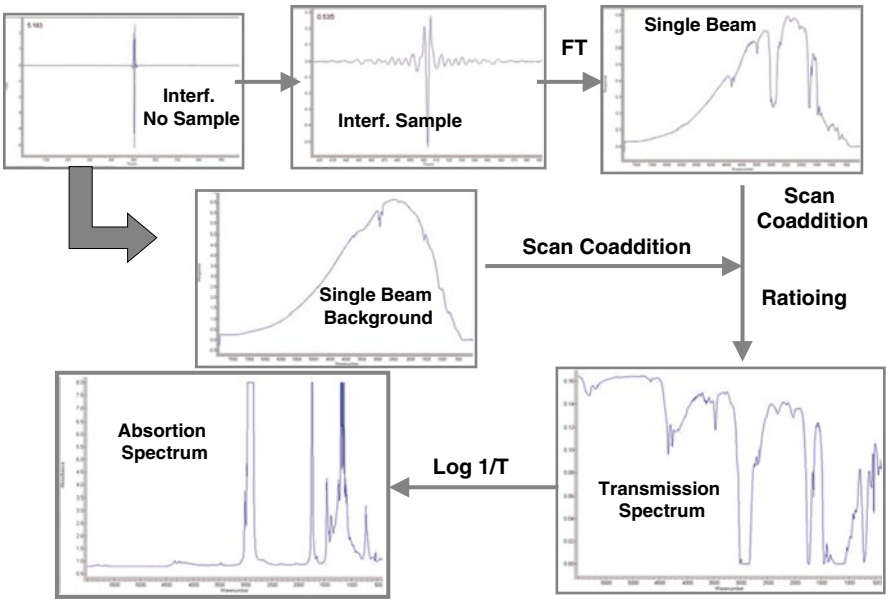

Fig. 10.4 Processing of signals in infrared spectroscopy from interferogram to absorption spectrum

the detector. The sample is introduced into the cell specially designed to have a constant sample thickness. Transmission cells are usually constituted by two crystal windows separated by spacers of different thicknesses, quartz cuvette of fixed thickness (e.g., 1 or 5 mm), or by disposable vials of fixed width (Williams and Norris 2001).

Transflection cells are designed for making transmittance measurements with instruments that are designed only to collect reflectance spectra (i.e., instruments where the source and the detectors are on the same side). A classic transflection cell is an aluminum cup covered with a slide glass (crystal or quartz) and having a gold plate as reflector. The energy traverses the sample once, is then reflected on the gold reflector, and traverses back to the sample before reaching the detector.

10.3.2 Mid-Infrared Spectroscopy

Until recently, MIR spectroscopy has been of limited use for the study of food materials due to a number of drawbacks. Food samples are often opaque and highly scattering. Furthermore, they often contain high concentrations of water, which absorbs strongly in the MIR region. Food materials, therefore, are not very

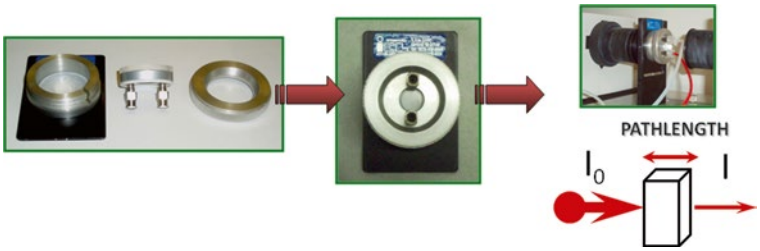

Fig. 10.5 Pictures of a typical transmission cell, demounted, assembled, and set up in FT-IR spectrometer

amenable to classic transmission techniques and sampling methods such as pellets or mulls (Wilson 1990). A second factor limiting the use of MIR spectroscopy with food samples has been that classic instrumental methods suffered from a lack of speed and from a low energy level of the sample due to the use of monochromators. However, the development of new sampling methods together with FT instruments have now made it possible to routinely analyze food samples by MIR spectroscopy (Wilson 1990; van de Voort and Ismail 1991).

The use of a Michelson interferometer allows much more energy to reach the sample, provides good wavelength reproducibility, and allows spectra to be collected in a very short time. Figure 10.4 shows the basic processing from the interferogram registered by a Michelson interferometer to transmission and absorption spectra. Apart from these combined advantages, it is worth noting that handle sampling is a major issue and is conditioned by the viscosity of the sample. FT MIR spectroscopy has made viable sample presentation techniques for edible oils, thus overcoming some of their analytical problems with MIR spectroscopy. The most important MIR sample presentation techniques applicable to oil analysis are transmission liquid cell and attenuated total reflectance (ATR) crystal, which are described in detail by Wilson and Goodfellow (1994). Both methods require a minimum of sample preparation.

10.3.2.1 Transmission Cells

Transmission cells allow for FT-IR analysis in transmission mode. In this mode the sample is located in the optical path of the IR beam (I_0). Figure 10.5 shows a typical transmission cell.

Liquid samples, such as virgin olive oil, are normally injected into the cell to form a thin-film squeezed between two windows. There are three main types of transmission cell, all employing metal frame plates, windows to enable light to enter and leave the sample, and spacers that define the optical path length (OPL). Thus, sealed cells employ permanently bonded spacers of a fixed thickness. This first type of cell is suitable for quantitative analyses, where an invariable OPL is required. The

Table 10.1 Main characteristics of window materials used for transmission cells in FT-IR spectroscopy

Window material	Working range (cm^{-1})	Refractive index	Advantages/disadvantages
NaCl	40,000–600	1.5	Low cost
			Highly hygroscopic; slightly soluble in alcohol; breaks easily
KBr	43,500–400	1.5	Low cost; good resistance
			Hygroscopic; soluble in alcohol and slightly in ether
KCl	33,000–400	1.5	Low cost
			Hygroscopic
CaF_2	77,000–900	1.4	Insoluble in water; resists most acids and bases; high hardness (suitable for high-pressure works)
			Expensive
BaF_2	66,666–800	1.5	Insoluble in water
			Soluble in acids and NH_4Cl; sensitive to mechanical shock
CsBr	42,000–250	1.7	Extended IR range
			Soluble in water and acids
CsI	42,000–200	1.7	Easier to handle than CsBr
			Hygroscopic; does not cleave; easily scratched
AgCl	25,000–434	2.0	Insoluble in water; inexpensive
			Darkens under UV radiation; corrosive to metals
KRS-5[a]	20,000–285	2.37	Insoluble in acids; does not cleave
			Slightly water soluble
ZnSe	10,000–555	2.20	Insoluble in water and weak acids and bases
			Expensive; brittle; must be handled with care
ZnS	10,000–714	1.5	Insoluble in water and weak acids
			Expensive; slightly soluble in acids (HNO_3, H_2SO_4, KOH)

[a]a mixed thallium bromide-thallium iodide

second kind, the demountable cells, may be dismantled to facilitate cleaning and enable the use of spacers with different thicknesses and, hence, different OPLs. Finally, piston cells enable the window separation to vary continuously over a range of OPLs. In any case, the OPL variations can be controlled by adding an internal standard with a known and distinct absorption (Ismail et al. 2006).

Liquid cells enable reasonable quantification of solute concentrations. Practical difficulties include the maintenance of a constant (repeatable) OPL and good window parallelism (to avoid wedging errors). The cell windows should be constructed from a material that is transparent to the MIR beam and, additionally, does not react with the samples. Thus, windows are commonly made of polished salt crystals (Table 10.1) that transmit IR radiation. Other materials with covalent bonds (e.g., glass) lack this property and, in consequence, cannot be used as window material. On the other hand,

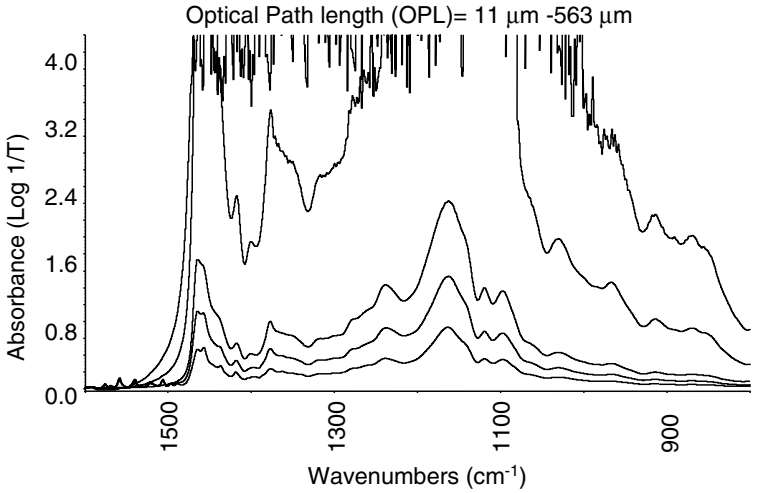

Fig. 10.6 Spectra of oils collected at different path lengths with KCl cell using spacers of several thicknesses (0.015–0.5 mm). Note: Spectra with larger OPL are off-scale

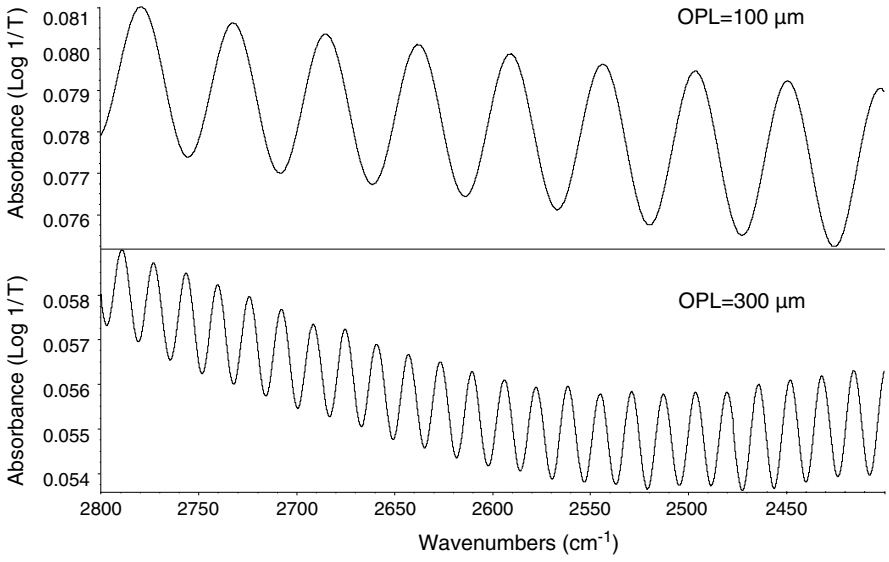

Fig. 10.7 Spectra collected from two empty transmission cells with optic path lengths (*OPL*) of 100 and 300 μm

given the limited energy provided by the IR source, strong absorbance by the solvent or nontarget chemicals may dominate the absorbance spectrum, obscuring weaker absorbance bands. Therefore, in some cases it is necessary to use very short OPLs (below 10 μm), which are difficult to produce and measure reliably.

One key aspect when operating with transmission cells in quantitative analysis is to know precisely the OPL to allow a correct calibration. The intensity of the IR spectral bands is determined by the OPL, which ultimately means the amount of sample between the two windows (Fig. 10.6). Then, an accurate quantitative analysis implies working under a constant and known OPL.

The procedure for determining the OPL is particularly important in demountable cells, and it should be carried out after cell assembly and prior to acquiring the spectra to make sure that no significant OPL change has resulted from the manipulation of the cell. One procedure consists in acquiring a spectrum with an empty cell. The spectrum (Fig. 10.7) recorded from the empty cell is characterized by a sinusoidal line with fringes (peaks) and valleys. The OPL is calculated by counting these interference fringes between two wavenumbers and applying the following equation:

$$OPL = \frac{n}{2(\overline{\nu}_2 + \overline{\nu}_1)},$$

where n is the number of peak-to-peak fringes, and

$\overline{\nu}_1$, $\overline{\nu}_2$ are the wavenumbers of the considered range.

Depending on the intensity of the IR band under study, the desirable OPL may lie below 100 μm. This short path length entails a difficult sample handling in the case of viscous liquids such as edible oils. For that reason, some new accessories have been designed for this particular case to ease sample loading (in the absence of bubbles) and cell cleaning. Thus, van de Voort (1994) developed a temperature-controlled transmission flow cell accessory that allows for the routine use of the FT-MIR technique in the quality controls of fats and oils. The instrument is composed of the basic FT-MIR spectrometer, a computer that controls the instrument, a temperature controller, the sample-handling accessory inlet, and control valves. All components of the sample accessory are heated (usually to 80 ± 0.2 °C) so that the sample can easily flow in the lines or the cell. The system includes a bypass line to flush out the bulk of the previous sample, which avoids having large samples pass through the cell and minimizes the cross contamination. In so doing, it is not necessary to clean the accessory between each spectral acquisition. In summary, an oil sample is heated in the test tube block, presented at the input line, and aspirated into the cell using the three-way valve.

Another approach to facilitate sampling of viscous oils is based on the concept of spectral reconstitution (SR) (van de Voort et al. 2007a). SR involves dilution with a less viscous liquid. The spectra of diluted samples are then converted into good facsimiles of the spectra of the neat oils, without a priori knowledge of the precise dilution factor. The dilution factor is calculated from an internal IR spectral marker

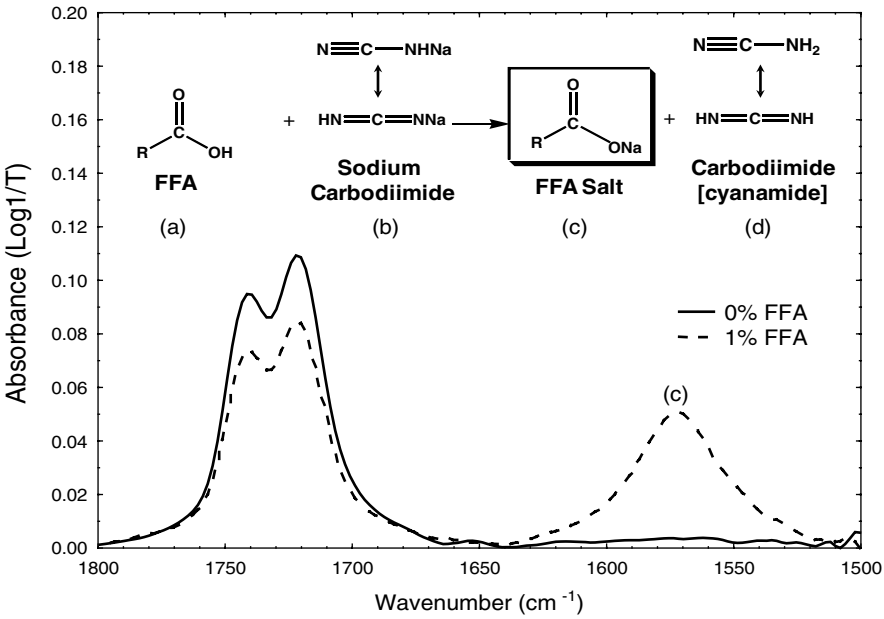

Fig. 10.8 Stoichiometric reaction associated with infrared analysis for free fatty acid (*FFA*) content and corresponding spectral changes taking place

that is added to the less viscous liquid and that does not interfere with the bands of the sample. The relation of the spectral bands of the marker in the less viscous liquid and the diluted samples gives information about the exact dilution factor (van de Voort et al. 2008). This procedure eliminates the need for a peristaltic pump, reduces sample volumes (from approximately 100 mL to approximately 5 mL), increases the number of samples per hour (up to 120 samples/h), and eliminates the need for solvent rinses, thereby drastically reducing disposal volumes.

The analysis of viscous samples with transmission cells can also be facilitated by the method of signal transduction-dilution. This method has been used mainly to measure acidity in mineral and edible oils (Li et al. 2009). In this procedure the chemical component to be characterized (e.g., acidity) is extracted with an oil-immiscible solvent (e.g., methanol) with a reagent (e.g., hydrogen cyanamide, NaHNC≡N) that reacts with the chemical component; this results in a measurable band. Figure 10.8 shows this stoichiometric reaction and the spectral changes that allow an accurate measurement of free fatty acid percentage. This procedure has been adapted to be performed in automated (Yu et al. 2009) and portable instruments (Li et al. 2008). The automated instrument (COAT, Thermal-Lube, Pointe-Claire, QC, Canada), also used with SR, includes a demountable IR cell, pumps, and valves to aspirate the samples, an autosampler for automated analysis, and a specific software (UMPIRE) that automatically analyzes different chemical features

Table 10.2 Commercial FT-IR sample cards and properties

Commercial name	Manufacturer/distributor	Film materials	Pathlength (μm)
3M IR cards[a]	3M	PE[b], PTFE[c]	10 and 100
PTFE and PTIR cards	International Crystal Laboratories	PE[b], PTFE[c]	Unknown
Real Crystal IR cards	International Crystal Laboratories	NaCl, KBr, KCl	Unknown
DOT.IR cards	PSI Performance Systematix	PTFE	Unknown
ST-IR cards	Thermo Scientific[d]	PE, PTFE	~10

[a]Discontinued
[b]Polyethylene
[c]Polytetrafluoroethylene
[d]Initially commercialized by Thermo Nicolet

and performs the mathematical operation necessary for SR (van de Voort et al. 2007b). On the other hand, the portable instrument (InfraSpec VFA-IR spectrometer, Wilks Enterprise, South Norwalk, CT) is a low-resolution IR spectrometer with no moving parts and an electronically modulated (pulsed) source combined with a linear variable filter mounted on a detector array (VFA). This instrument has also been used coupled with an attenuated total reflection accessory in addition to transmission cells.

Although transmission cells provide a wide range of possible applications, some adaptation and new designs have been presented for a better performance in particular cases. One of these modifications involves the hyphenation of a FT-IR spectrometer and another technique. Transmission flow cells are easier to hyphenate to other techniques in comparison with other FT-IR accessories. Thus, several systems have been mounted to connect a separative technique (e.g., HPLC or GC) to a transmission cell and a FT-IR detector (Vonach et al. 1997; Ahro et al. 2002; Kuligowski et al. 2010). Another modification in the cell is the inclusion of a heater to study the oxidative behavior of edible oils (Ismail et al. 2006), also used in NIR spectroscopy (Gonzaga and Pasquini 2006). The oxidation of edible oils has also been used in disposable cards, whose design is somewhat inspired by classic transmission cells.

10.3.2.2 Disposable IR Cards

Table 10.2 shows a summary of commercial FT-IR cards. The disposable IR cards were developed in the 1990s by 3M for the analysis of liquids or spreadable fats. The cards are made up of a cardboard holder containing a circular IR-transmitting window made of a microporous substrate (polytetrafluoroethylene substrate for 4,000–1,300 cm^{-1} or polyethylene substrate for 1,600–400 cm^{-1} MIR analysis), although some manufacturers are commercializing cards of other materials. The sample is adsorbed on the mycrocrystaline pores of the film material, resulting in an

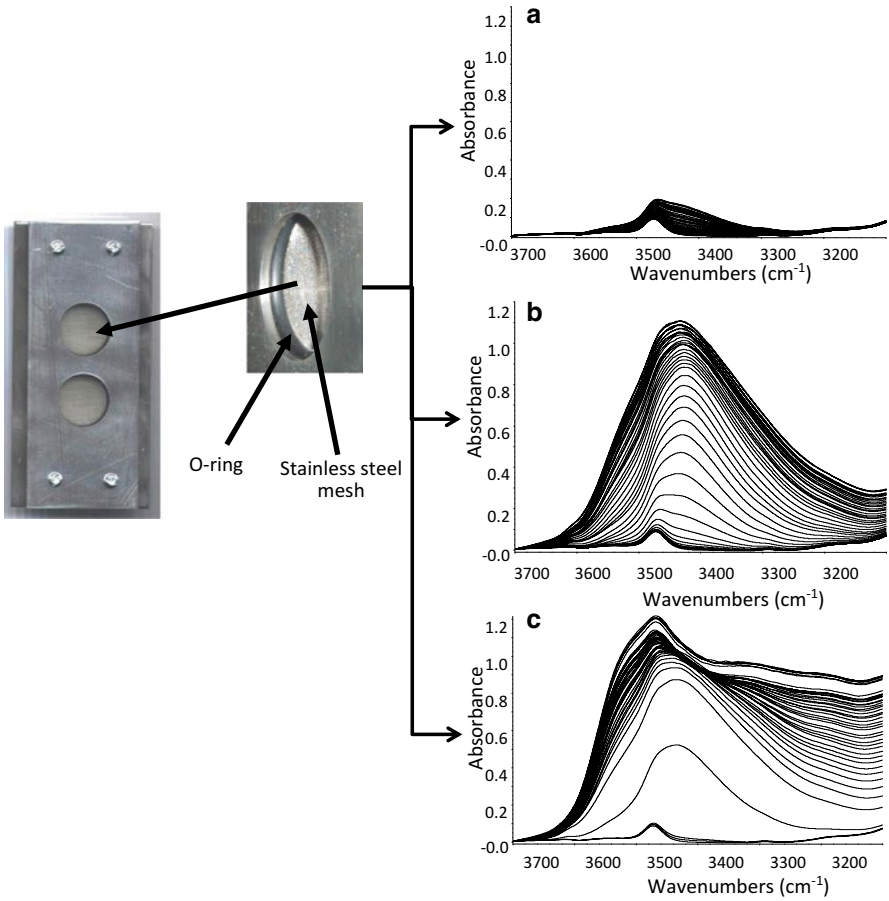

Fig. 10.9 Design of stainless steel mesh cell for infrared spectroscopy and spectra on OH stretching region (3,700–3,100 cm^{-1}) for canola oil in a mesh cell over a period of 42 days kept in the dark (**a**), exposed to room light (**b**), and heated at 50 °C (**c**) (*Source*: García-Gonzàlez and van de Voort (2009), with permission of Applied Spectroscopy)

effective path length of approximately 100 μm. The substrate bands of the microporous material can be subtracted from the sample spectra. A nonporous ring around the aperture prevents the sample from being absorbed by the cardholder. These cards were successfully applied to determine *trans* fatty acid content and the peroxide value (PV) of edible oils (Ma et al. 1998, 1999). Another type of IR cards (Type 2 STIR-PIR cards, Thermo-Nicolet) allows even shorter path lengths but lacks the nonporous ring around the aperture, and in consequence there is not consistency over time.

An improved version of these IR cards is the IR mesh cell (García-González and van de Voort 2009) (Fig. 10.9). Although it can be used for general applications, this

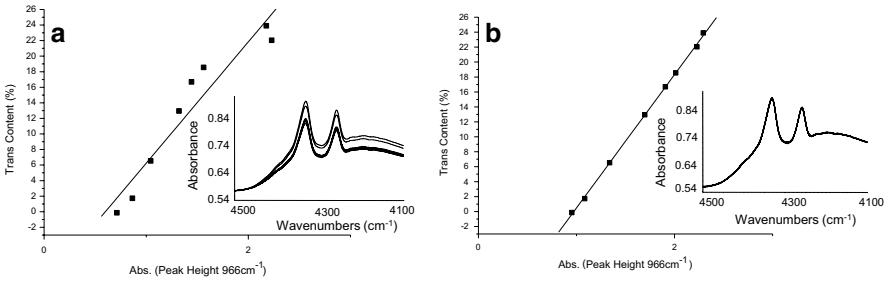

Fig. 10.10 Regression lines relating *trans* fatty acid content and peak height of 966 cm^{-1} band. (**a**) Data without normalization; (**b**) data normalized using CH overtone band at 4,334 cm^{-1} (shown in each panel as an inset) (*Source*: García-Gonzàlez and van de Voort (2009), with permission of Applied Spectroscopy)

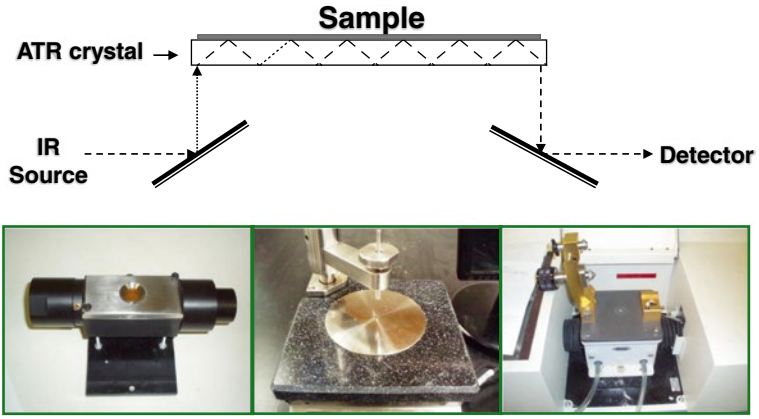

Fig. 10.11 Scheme of working principle of attenuated total reflectance (*ATR*) and three pictures of typical ATR accessories

cell is particularly adequate for running oxidation at moderate temperatures in a wide variety of conditions. The design of this new cell enables one to obtain a fairly consistent path length during the entire time of the experiment. This cell is endowed with a mesh that entraps the oil sample by means of its inherent surface tension. The high surface area provided by the mesh facilitates the rapid oxidation of the oil by air at ambient or slightly elevated temperatures with no need of extreme temperature conditions. These mesh cells are not disposable and can be easily cleaned and reused. Although the effective path length is fairly consistent over the course of the experiment, small changes in the sample thickness can been corrected using the CH combination band region (4,500–4,100 cm^{-1}) as a reference band (García-González and van de Voort 2009). This band provides information on the CH double bonds and, thus, on the amount of sample and the OPL. This normalization procedure makes it possible to obtain reproducible spectra despite the small changes in the OPL

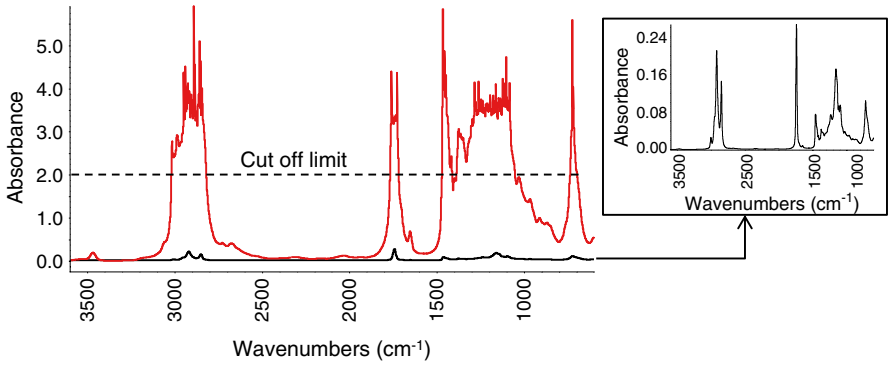

Fig. 10.12 Spectra of an oil collected with an ATR accessory (*black line*) and a transmission cell (*red line*)

over time or between different mesh cells. Thus, Fig. 10.10 shows the significant improvement in *trans* fatty acid calibration when the spectra have undergone normalization by the CH combination band.

10.3.2.3 Attenuated Total Reflectance (ATR)

Methods based on the ATR principle are available in a diverse range of configurations and optical designs. They typically require minimal sample presentation and are particularly suited to study highly absorbing samples such as edible oils. The spectral information arises from the interaction between the sample and the evanescent wave produced in an internal reflectance element (IRE). Infrared light is sent to the crystal at such an angle that it becomes internally reflected. Figure 10.11 shows a scheme of the working principle as well as some examples of ATR accessories, either multibounce or single-bounce (depending on the number of beam reflections within the ATR crystal).

Depending on the geometry and length of the crystal, the light will undergo multiple reflections before emerging from the crystal. At each reflection an evanescent wave is established that decays exponentially into the medium in contact with the crystal. If this medium is absorbing, then there will be a transfer of energy from inside the crystal to the surrounding medium and the emerging beam will be attenuated. ATR does not rely on the sample, which constitutes the surrounding medium, which is transparent or transmitting in the conventional sense (Harrick 1967).

ATR allows opaque or highly scattering samples to be used; the only proviso is that the sample must make intimate contact with the ATR crystal. This condition is fully completed with oil samples. The effective penetration (OPL) at any reflection is very short, typically a few microns, so that ATR can be used to overcome the strong absorption of materials. Thus, unlike the spectra obtained with transmission cells, ATR spectra have no cutoff limit or saturation problem and is suitable to study the whole spectra including the most intense bands (Fig. 10.12). A short effective

path length is obtained with no restrictions on the sample thickness, so the sample is simply poured onto the ATR crystal. The optical paths are very reproducible from one sample to another. ATR then allows easy sample measurement, which is one reason that there has been an upsurge in interest in the MIR region (Wilson 1990). ATR crystals should be constructed from a material with a high refractive index, which is highly transmitting, inert, robust, easily cleaned, and resilient to abrasion and corrosion (including dissolution). Classically horizontal ZnSe, Ge, Si, or diamond crystals with 1, 6, or 12 internal reflections are used in oil analysis (van de Voort 1994a; Baeten et al. 2005; Abbas et al. 2009). Some disadvantages of ATR analysis are the low sensitivity because of the short effective path length (weak bands need to be studied with transmission cells), the significant effect that contaminations on the crystal might have on the collected spectra, and the need for temperature control (the depth of penetration of the IR beam depends on temperature) (Ismail et al. 2006).

10.3.3 Raman Spectroscopy

In the past, the application of Raman spectroscopy in food science was considered to be of very limited use because of fluorescence interference, photodecomposition, wavelength calibration, lack of precise frequency base from scan to scan, and the difficulty of attaining high-resolution spectra with the classic dispersive Raman spectrometer (Chase 1987). However, major instrumental advances have contributed to the widespread use of Raman spectroscopy in recent years (Gerrard and Birnie 1992) and its application in food science (Ozaki et al. 1992; Keller et al. 1993; Li-Chan 1996, 2010a).

First was the demonstration, by Hirschfeld and Chase in 1986, that Raman spectra could be obtained with a FT spectrometer equipped with a Nd:YAG laser (NIR monochromatic light excitation), a Rayleigh rejection filter, and a germanium detector. Later on, the development of compact and reliable diode lasers improved the quality of the commercially available systems. A third contribution to these developments was the use of low-noise, multichannel coupled charge device (CCD) detectors. By coupling the appropriate laser and a CCD detector to a spectrograph, it is now possible to measure Raman spectra in a few seconds without exciting fluorescence. Commercial FT-Raman spectrometers offer a good signal-to-noise ratio, a high IR-light throughput, rapid analysis, and the accuracy of wavelength calibration (Levin and Lewis 1990; Diem 1993; Schrader 1996; Li-Chan et al. 2010a).

FT-Raman spectroscopy is arguably the most versatile and easy-to-use nondestructive analytical procedure developed. In fact, glass and water have a very weak Raman spectrum, making the technique even easier to use. Samples can be measured directly in the bottle in the case of an oil. In addition, a spherical cell, such as a nuclear magnetic resonance (NMR) tube, allows Raman scattering information to be collected easily and rapidly (Schrader 1996). On the other hand, if samples to be investigated cannot be transported to the spectrometer, then optical fibers can be

used (as in NIR spectroscopy). In the range of FT-Raman spectroscopy, quartz fibers have very high transmittance (Lewis et al. 1988; Hendra et al. 1997).

10.3.4 Fluorescence Spectroscopy

Fluorescence spectroscopy, like other vibrational spectroscopic techniques, is characterized by its simplicity of sample presentation. To obtain a fluorescence spectrum, it is necessary to excite a sample with an energy-specific excitation wavelength (λ_{ex}), which comes from an excitation source, passes through a filter or monochromator, and strikes the sample. Then a fluorescent light is emitted in all directions. Some of this fluorescent light passes through a second filter or monochromator, dividing the light into different emission wavelengths (λ_{em}), which reach a detector.

There are two general types of instruments: filter fluorometers, which use filters to isolate the incident light and flourescent light, and the most common spectrofluorometers, which use diffraction grating monochromators to isolate the incident light. Both types of instrument are composed of excitation sources, normally a xenon lamp, filter or monochromator in excitation, filter or monochormator in emission, and a detector. The detector is usually placed at 90° to the incident light beam to minimize the risk of transmitted or reflected incident light reaching the detector. The detectors can be classified as single-channel or multichannel. The difference between them is based on the number of wavelengths that they can detect at a time. Thus, the single-channel detector can only detect the intensity of one wavelength at a time. In contrast, the multichannel type detects the intensity at all wavelengths simultaneously.

Various light sources may be used as excitation sources, including lasers, photodiodes, and lamps such as xenon arcs and mercury-vapor lamps. Of these, only the xenon arc lamp has a continuous emission spectrum, with nearly constant intensity in the range of 300–800 nm and a sufficient irradiance for measurements down to just above 200 nm.

The most common accessory used to analyze the fluorescence spectrum of liquid samples, and vegetable oils in particular, are quartz cuvettes with different paths, internal widths, and volumes.

In addition to the conventional collection of emission spectra with a single excitation wavelength, some fluorometers can be adapted to conduct analyses under two particular modes that provide some advantages over the conventional mode. These particular ways of measuring are commonly known as excitation-emission florescence spectroscopy (EEFS) and synchronic fluorescence spectroscopy (SFS).

10.3.4.1 Excitation-Emission Fluorescence Spectroscopy (EEFS)

EEFS consists in measuring the emission spectra at different excitation wavelengths (λ_{ex}). The result of this measurement is a three-dimensional (3D) excitation-emission matrix (EEM). Compared to conventional fluorescence spectroscopy, this technique improves the selectivity of the method. Its main advantage is that it enables obtaining simultaneous information about the different fluorophores present in a sample. Furthermore, EEFS is useful for selecting the most convenient excitation wavelengths to study specific fluorescent compounds in complex matrices by conventional fluorescence spectroscopy. The measurements under this mode also have some disadvantages. The spectroscopic parameters must be optimized beforehand to avoid Rayleigh scattering caused as a result of the overlap between the ranges of wavelengths of excitation and emission. As a drawback, this mode consumes a longer analysis time to obtain a matrix (EEM), approximately 10 min depending on the spectral ranges used. The statistical data treatment is also more sophisticated or requires a preliminary decomposition of the information EEM in two-dimensional arrays. For this purpose, parallel factor analysis (PARAFAC) is an appropriate way to decompose and interpret 3D data matrices (Tena et al. 2012).

10.3.4.2 Synchronous Fluorescence Spectroscopy (SFS)

This technique consists in scanning the signal of two monochromators, the excitation and emission, simultaneously, keeping a constant interval of wavelengths ($\Delta\lambda$) between excitation (λ_{ex}) and emission (λ_{em}) wavelengths. Three types of SFS procedures can be distinguished depending on the scan rate: (1) constant-wavelength SFS, where the interval wavelength ($\Delta\lambda$) between λ_{ex} and λ_{em} is kept constant; this is the most widely used SFS procedure; (2) constant-energy SFS, where a frequency difference ($\Delta\upsilon$) is kept constant; (3) variable-angle SFS, where the excitation and emission wavelengths may be varied simultaneously but at different rates. These last two types are more difficult to implement, mostly because commercial fluorimeters are not endowed with the necessary software for such scans. Thus, a regular fluorimeter typically only allows a constant-wavelength SFS. The selection of $\Delta\lambda$ depends on which fluorophore compounds comprise the analytical targets of the study. Most of the reviewed literature on SFS indicates that 3D rendering helps in obtaining a better characterization of multifluorophore systems. The resulting 3D surfaces are obtained when the ZZ' axis is represented – the different wavelength intervals ($\Delta\lambda$) used in the course of the experiments – versus the XX' axis, which represents the range of synchronous wavelengths scanned. This graph is used to determine which $\Delta\lambda$ is the most appropriate for obtaining more information about particular spectral bands.

One advantage of total SFS is the narrowing of the bands, which simplifies the spectrum by minimizing the spectral overlap. This narrowing of bands depends on the selected wavelength interval ($\Delta\lambda$). The high selectivity of the total synchronous fluorescence spectra makes this technique suitable for the qualitative analysis of complex samples. The main disadvantages of this mode are the difficulty of selecting an appropriate $\Delta\lambda$ in the case of multicomponent samples and the requirement of specific instrumentation and software to take full advantage of the technique (monochromator plus driving software).

10.3.5 Online Analysis

In the food industry, monitoring of the process is a major issue in order to optimize it and to assure the quality of the end products. To this end, at-line or online analytical methods can be applied. With at-line methods, samples are taken from the process line and analyzed close to it or in a laboratory. At-line methods are time-consuming and do not allow one to obtain the required information in due time in order to act rapidly (or even instantaneous) on the process. Online methods, where the instrument is directly installed in the process line, is more appropriate for process monitoring. NIR, MIR, and Raman spectroscopy are techniques that are suitable for providing real-time measurements that can be integrated into an industrial process. Recent developments have been observed mainly in the setup of adequate sensors and software allowing the collecting of spectral information and to use it to pilot food processes. Online NIR spectroscopy has several advantages, such as speed of measurement, well-developed equipment and devices, absence of a need for sample preparation as well as analysis of simultaneous parameters. The main disadvantage is the need for robust calibrations and model transfer between instruments (Kondepati and Heise 2008). The online applications of NIR in food systems have recently increased significantly. Huang et al. (2008) published a review on NIR online analysis of foods such as meat, fruit, grain, dairy products, and beverages. Online MIR spectroscopy is less frequently used in the food industry but has several advantages over NIR spectroscopy such as high sensitivity, ability to distinguish between very similar structures, and good calibration transfer between instruments. Online MIR application suffers mainly from the strong absorption of water and the high cost (e.g., fiber optics suitable for MIR analysis are more expensive and less adapted for online control than those suitable for NIR analysis). Few studies on the use of MIR for online applications, such as monitoring a fermentation reaction, have been reported (Bellon-Maurel et al. 1994; Fayolle et al. 2000). Unlike MIR online spectroscopy, online Raman spectroscopy has few applications

in the food industry. However, it is commonly used in the pharmaceutical processing industry.

Few papers dealing with online use of NIR spectroscopy for the control of olive oil, olive pomace, and olive paste have been published. One of the first preliminary studies of the application of online NIR spectroscopic methods in this field was published by Hermoso et al. (1999). In this paper, the NIR technique was used to measure the oil content and humidity in olive pomace at the decanter. The study provided determination coefficients of 0.91 and 0.6 between NIR spectroscopy and the reference values of oil content and humidity obtained by NMR and the drying-oven method, respectively. Jiménez-Márquez et al. (2005) applied NIR transmittance spectroscopy to characterize virgin olive oils. Partial least-squares (PLS) models were developed for acidity value, bitter taste, and fatty acid composition. Gallardo-González et al. (2005) used NIR to determine in real time the moisture and fat contents of olive pastes and the resulting olive wastes generated in the two-phase oil extraction process. Coefficients of determination of 0.90 for humidity and 0.91 for oil content in olive paste samples were obtained.

More recently, some authors (Cayuela et al. 2009; Cayuela and Pérez-Camino 2010) predicted olive fruit and virgin olive oil parameters by directly measuring the fruit using NIR. The analyzed parameters were free acidity in olive oil, oil yield from physical extraction, oil content referring to fresh weight, oil content referring to dry matter and fruit moisture. The results indicated a very good predictive potential of the methodology and served to encourage improvement in the obtained models through the enlargement of calibration databases and models.

10.4 Data Acquisition

The data acquisition procedure in IR or Raman spectrometry is not tedious and can be done by nonskilled technicians. Basically, the principal steps are as follows: preliminary work for data acquisition (e.g., cool the detector with N_2 in Raman spectroscopy, heat the sample accessory in NIR or MIR spectroscopy), instrument performance verification, stabilization, and data collection. These steps are, for the most part, described in the technical manual supplied with the instrument. The performance of the instrument is generally checked by various automatic functions that are included in the program designed to control the spectrometer. However, before each experiment, it is appropriate to collect and store the spectrum of a defined standard (e.g., oil or chemical product defined as standard). In so doing, the spectral quality and the stability of the spectrometer can be verified each day.

The stabilization procedure is essential for acquiring a high-quality spectrum, i.e., a spectrum with a good signal-to-noise ratio. The manual of the instrument will contain the reference value normally reached by the spectrometer. To perform this work, the more convenient way is by successively collecting the spectral data of the

same sample. It is important to do this collection under conditions that will be used in practice. The acquisition of a series of spectra before the analytical step allows, according to the analytical conditions, the stabilization of the instrumental components (e.g., source, detector). The analytical conditions include the number of scans to coadd and the resolution of the spectrum. The best way to define these parameters is to carry out a repeatability study, changing one of the parameters at a time. In comparison to simple univariate analysis, little progress has been made so far in the quantification of variability in multivariate analysis. Hence, it is judicious to complete the statistical results from the univariate analysis (SD and CV) with those from a multivariate procedure such as cluster analysis. Cluster analysis develops a mathematical model evaluating the similarities and dissimilarities between multivariate data (Massart and Kaufman 1983). A convenient agglomerative procedure and linkage distance in the analysis of spectroscopic data are Ward's method and the city-block (Manhattan) distance, respectively (Chap. 12). A low value of the linkage distance indicates a high similarity, i.e., a good repeatability.

When the instrument performance has been checked and the stability of the instrument achieved, the data collection procedure can be carried out. This step includes the reference spectrum acquisition, the sample spectrum acquisition, and sample-handling cleaning. The reference spectrum consists of the spectrum of the empty sample accessory or the spectrum of a reference compound (e.g., ceramic plate in NIR spectroscopy). This step permits the removal of absorbances due to the instrument and sample handling used from the sample. Depending on the technique and the sample accessory used, the reference spectrum should be collected once a day (e.g., NIR) or before each spectral data acquisition (e.g., ATR/FT-MIR). After the reference acquisition, the sample is introduced in the sample accessory and its spectrum is collected. Before the following data acquisition, the sample must be removed and the accessory cleaned (this is not the case with automatic sampling methods, as discussed in Sect. 10.3.2.). Then, the cleaned sample handling should be spectrally checked to ensure that no residue from the previous sample remains.

10.5 Interpretation of Oil Spectra

The most frequently discussed drawback of spectroscopic techniques is the difficulty of chemically interpreting the spectral data. Separative techniques like chromatography generate information (chromatograms) mainly containing well-resolved and separate peaks, i.e., discrete information. Infrared and Raman spectroscopic techniques generate continuous information (spectra) rich in both isolated and overlapping bands. While in chromatography each peak is, in general, characteristic of a precise compound, in spectroscopy, the bands are the result of the vibration of one or more chemical bonds (e.g., C-H, C=C) present in all the compounds constituting

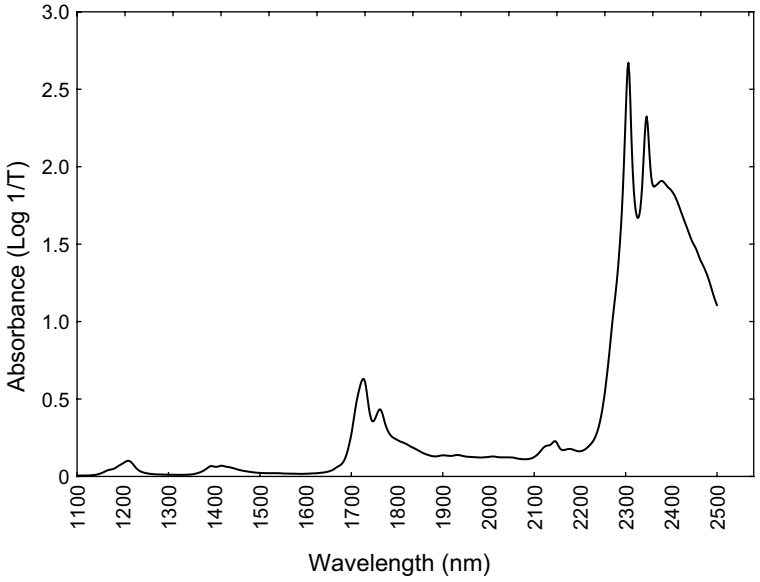

Fig. 10.13 Near-infrared spectrum of a virgin olive oil

the sample. Each band in the spectrum of a mixture contains the sum of the information of various molecules.

To make up for the unreadable information on the IR and Raman spectra, it is important to study the spectral features of pure chemical products. Edible oils mainly contain triacylglycerols (TAGs) whose types and proportion vary according to their source. Hence, the study of pure compounds such as TAGs (or fatty acid methyl esters) allows the band assignment of the principal absorption (NIR, MIR) or scattered (Raman) bands observed in the spectra. Various papers have presented the spectral features of pure chemical products (Holman and Edmondson 1956; Bailey and Horvat 1972; Sadeghi-Jorabchi et al. 1991; Sato et al. 1991; van de Voort et al. 1994b; Hourant et al. 2000; Baeten et al. 2001; Stefanov et al. 2010). In addition, various companies offer spectral libraries containing the characteristic spectra of the compounds concerned.

The analysis of various kinds of samples from different animal and vegetable sources permits the interpretation of the most noteworthy bands. The correlation at each frequency between the absorption (or scattering) intensity and chemical compounds (or indices) can be calculated using the fatty acid profile determined by gas chromatography. These correlation graphs help the analyst to underline the spectral features of each oil source and guide the subsequent data analysis.

To present the main characteristics of NIR, MIR, and Raman spectra, the relevant frequencies of pure chemical compounds will be presented and discussed later on. For

Table 10.3 Assignment of most noteworthy near-infrared absorption bands of a virgin olive oil spectrum

Wavelength (nm)	Molecule	Group	Vibration
1,090–1,180	$-CH_2$	C-H	Second overtone
1,100–1,200	$-CH_3$	C-H	Second overtone
1,150–1,260	-CH=CH-	C-H	First overtone
1,350–1,430	$-CH_2$	C-H	Combination
1,360–1,420	$-CH_3$	C-H	Combination
1,390–1,450	H_2O	O-H	First overtone
1,650–1,780	$-CH_2$	C-H	First overtone
	$-CH_3$	C-H	First overtone
	-CH=CH-	C-H	First overtone
1,880–1,930	H_2O	O-H	Combination
2,010–2,020	-CH=CH-	C-H	Combination
2,100–2,200	-CH=CH-	C-H	Combination
2,240–2,360	$-CH_3$	C-H	Combination
2,290–2,470	$-CH_2$	C-H	Combination

Table 10.4 Relevant near-infrared wavelengths (nm) of several lipids and bands that are correlated with some chemical indices (R>0.90)

	Spectral region		
Lipids	Second overtone	First overtone	Combination
Tricaprin (C10:0)		1,726, 1,800	2,128
Triolein (*cis* C18:1)		1,725	2,143
Trilinolein (*cis* C18:2)		1,665, 1,717	2,143
Trilinoelaidin (*trans* C18:2)		1,725, 1,800	2,131
Trilinolenin (*cis* C18:3)		1,665, 1,712	2,143
MUFA		1,724, 1,766	2,358
PUFA	1,162, 1,212[a]	1,660, 1,698, 1,730[a]	2,136, 2,176, 2,224, 2,310[a], 2,348[a], 2,434[a]
IV	1,164	1,664, 1,714, 1,740[a], 1,784[a]	2,144, 2,178, 2,340[a], 2,444[a]

UFA unsaturated fatty acids, *MUFA* monounsaturated fatty acids, *PUFA* polyunsaturated fatty acids, *SFA* saturated fatty acids, *IV* iodine value
[a]negative correlation coefficient

each technique, the principal correlated frequencies with the total amount of unsaturated fatty acids (UFA=C16:1+C18:1+C18:2+C18:3), monounsaturated fatty acids (MUFA=C16:1+C18:1), polyunsaturated fatty acids (PUFA=C18:2+C18:3), saturated fatty acids (SFA=C6+C8+C10+C14+C16+C18), and iodine value (IV=1*C 16:1+1*C18:1+2*C18:2+3*C18:3) are displayed in the next paragraph.

Table 10.5 Assignment of most noteworthy mid-infrared bands of a virgin olive oil spectrum

Wavenumber (cm^{-1})	Molecule	Group	Vibration
3,007	*cis* -CH=CH-	C-H	ν
2,955	$-CH_3$	C-H	ν
2,924	$-CH_2$	C-H	ν
2,855	-CH2 and $-CH_3$	C-H	ν
1,746	-C=O	C=O	ν
1,653	*cis* -CH=CH-	C=C	ν
1,462	$-CH_2$	C-H	δ
1,377	$-CH_3$	C-H	δ
1,236	$-CH_2$	C-H	δ
1,300–800	Carbon skeleton	C-C	δ
1,200–1,000	-CO-O-	C-O	δ
990–960	*trans* -CH=CH-	C-H	δ
723	$-CH_2$	C-H	δ

ν stretching, δ deformation

10.5.1 Near-Infrared Spectra

NIR spectra show various overlapping peaks. As seen in the theory section, these bands are the result of overtones (first and second) and a combination of fundamental, largely hydrogenic, vibrations that occur in the MIR region. Various books and papers describe the assignment of the major NIR absorption bands (Holman and Edmondson 1956; Goddu 1957; Fenton and Crisler 1959; Williams and Norris 2001; Panford and deMan 1990; Sato et al. 1991; Sato 1994). Figure 10.13 and Table 10.3 display, respectively, the NIR spectrum (1,100–2,500 nm) obtained with a transmission cell and the assignment of the most noteworthy absorption bands of a virgin olive oil.

All studies that have used the NIR region of the electromagnetic spectra have shown that oil spectra contain information about the degree of unsaturation (IV) (Holman and Edmondson 1956), the total unsaturation (Goddu 1957), the carbon number (Wetzel 1983), and the composition of the unsaturated fraction (Sato et al. 1991). In addition, NIR spectra show specific information about *cis* isomers, while *trans* isomers have no noteworthy bands.

Sato et al. (1991) showed that mainly two regions of the NIR spectra have particular features (Table 10.4). First, an absorption intensity near 1,720 nm is characteristic of the first overtone of the C-H vibration of various chemical groups ($-CH_3$, $-CH_2$, =CH-) and varies according to analyzed TAGs. In fact, as the degree of unsaturation increases, the maximum point observed in the spectra of triolein at 1,725 nm shifts to 1,717 nm and 1,712 nm in spectra of trilinolein and trilinolenin, respectively. Second, the absorption band in the area of 2,143 nm, characteristic of the C-H vibration of *cis*-unsaturation, is more intense in polyunsaturated than in monounsaturated fatty acid spectra. Saturated and *trans* fatty acids show weak peaks and

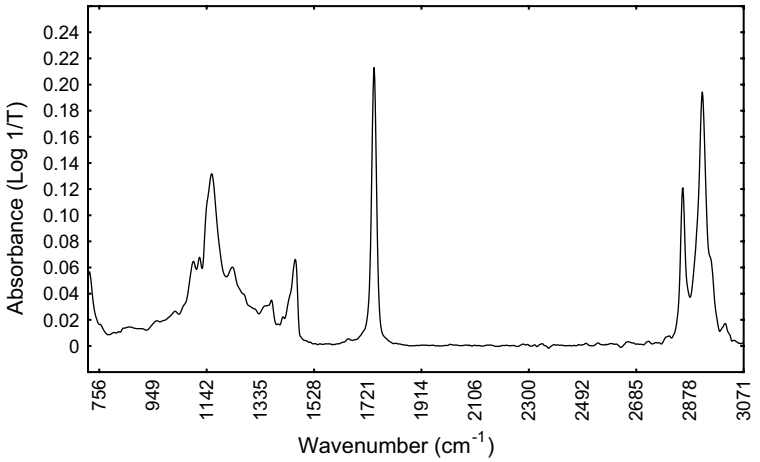

Fig. 10.14 FT-mid-infrared spectrum of a virgin olive oil

with maxima in the vicinity of 2,128 and 2,131 nm. Wavelengths in the region of 1,800 nm seem to be characteristic of saturated fatty acids.

A study of 104 samples from 18 different sources (animal and vegetable) showed that the spectral features of oils and fats agree with their fatty acid composition as determined by gas chromatography (Hourant 1995; Hourant et al. 2000). Oils with a high amount of polyunsaturated fatty acids have a maximum absorption band at lower wavelengths in the vicinity of 1,720 nm. Moreover, they have higher absorbance intensity, in the vicinity of 1,720 and 2,140 nm, than oils rich in monounsaturated fatty acids. Sunflower, walnut, and soybean oils present a maximum intensity near 1,720 nm, corn and rapeseed oils near 1,722 nm, and peanut, high oleic sunflower, and olive oils in the vicinity of 1,724 nm. The spectral regions 1,100–1,300 and 2,050–2,230 nm also show spectral features characteristic of these vegetable species. Table 10.4 regroups the wavelengths showing a high coefficient of correlation (greater than 0.90) between the absorption intensities and different chemical indices.

10.5.2 Mid-Infrared Spectra

A MIR spectrum of vegetable oil contains well-resolved peaks (3,100–1,700 cm^{-1}) and overlapping peaks (fingerprint region, 1,500–700 cm^{-1}) whose assignment is more difficult (Socrates 1994). Figure 10.14 displays the MIR spectrum of virgin olive oil, while Table 10.5 shows its most noteworthy bands (Fig. 10.14).

Based on the information contained in the MIR spectra, a series of methods has been developed to quantify the *trans* content (AOCS 1988; Sleeter and Matlock 1989; Ulberth and Haider 1992; van de Voort et al. 1995; Mossoba et al. 1996;

Table 10.6 Relevant mid-infrared wavenumbers (cm^{-1}) of several lipids and bands that are correlated with some chemical indices (R>0.90)

	Spectral region	
Lipids	= C-H stretching	Fingerprint region
Tristearic (C18:0)	–	–
Triolein (*cis* C18:1)	3,005	913
Trielaidin (*trans* C18:1)	3,025	966
Trilinolein (*cis* C18:2)	3,010	913
Trilinoelaidin (*trans* C18:2)	3,025	968
Trilinolenin (*cis* C18:3)	3,012	913
MUFA	3,011, 2,964	1,425, 1,396, 1,273, 1,134, 1,101, 914
PUFA	2,924, 2,854	1,464, 1,408, 1,313, 1,118
IV	3,011, 2,965, 2,922[a], 2,853[a]	1,429, 1,395, 1,267, 1,132, 1,117[a], 1,098, 922

UFA unsaturated fatty acids, *MUFA* monounsaturated fatty acids, *PUFA* polyunsaturated fatty acids, *SFA* saturated fatty acids, *IV* iodine value
[a]negative correlation coefficient

Ratnayake and Pelletier 1996), the *cis* content (van de Voort et al. 1995), the peroxide content (van de Voort et al. 1994b), the aldehyde content in thermally stressed oils (Dubois et al. 1996), and the free fatty acid content (Ismail et al. 1993). MIR spectroscopy was also used in the determination of indices such as the anisidine value (Dubois et al. 1996), iodine value (Afran and Newberry 1991; Muniategui et al. 1992; van de Voort et al. 1992), saponification number (van de Voort et al. 1992), and the solid fat index (van de Voort et al. 1996).

The investigation of pure fatty acids underlines the fact that spectral features change with the degree of unsaturation (van de Voort et al. 1995). The C-H stretching vibration of $-CH_2$ and $-CH_3$ groups (2,950–2,800 cm^{-1}),the C=O stretching vibration of carbonyl groups (1,745 cm^{-1}), and the C-H bending vibration of $-CH_2$ and $-CH_3$ groups (1,400–1,200 cm^{-1}) have absorption band intensities that change with the degree of unsaturation of the lipid matter. Moreover, the peak centered near 3,005 cm^{-1} (C-H stretching vibration of *cis* -CH=CH-) in the spectrum of triolein shifts to higher frequency in the trilinolein (3,010 cm^{-1}) and trilinolenin (3,012 cm^{-1}) spectra as the degree of unsaturation rises (Table 10.6). On the other hand, *trans* fatty acids show a peak centered near 3,025 cm^{-1}.

The fingerprint region of pure fatty acids is rich in features indicative of the degree of unsaturation, the type of unsaturation (mono- or polyunsaturated), or the content of *cis* and *trans* isomers. In a range from 1,125 to 1,095 cm^{-1} (characteristic of C-O and C-C stretching vibration), the peak intensities and the shape of the spectra vary with the unsaturation of fatty acids.

A study of 64 samples from 13 sources revealed that certain absorption bands of oil spectra vary with their fatty composition (Hourant 1995). The weak peak near 3,010 cm^{-1} has a higher intensity as the major fatty acids in the sample are monounsaturated or polyunsaturated. Moreover, samples rich in C18:1 (e.g., olive oil) have higher absorbance near 2,953 and 2,922 cm^{-1} than those rich in C18:2.

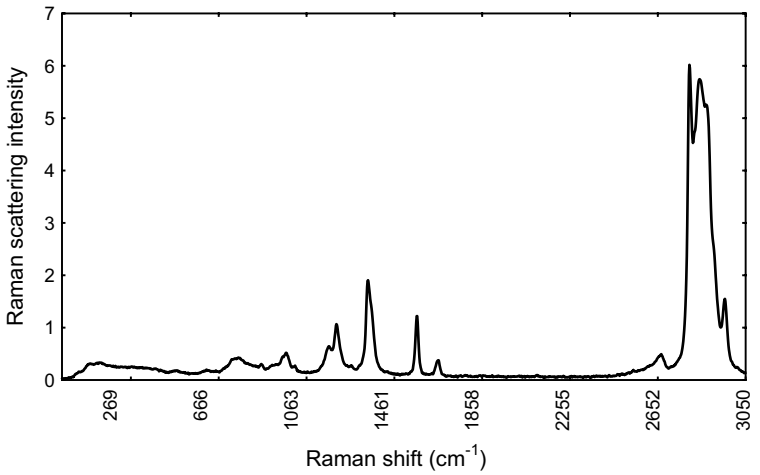

Fig. 10.15 FT-Raman spectrum of a virgin olive oil

Table 10.7 Assignment of most noteworthy Raman scattering bands of a virgin olive oil spectrum

Raman shift (cm^{-1})	Molecule	Group	Vibration
3,007	RCH=CHR	=C-H	ν
2,926	$-CH_2$	C-H	ν
2,897	$-CH_3$	C-H	ν
2,855	$-CH_2$	C-H	ν
1,748	RC=OOR	C=O	ν
1,670	*trans* RCH=CHR	C=C	ν
1,655	*cis* RCH=CHR	C=C	ν
1,441	$-CH_2$	C-H	δ
1,306	$-CH_2$	C-H	δ
1,270	*cis* RCH=CHR	=C-H	δ
1,100–1,000	$-(CH_2)_n-$	C-C	ν
900–800	$-(CH_2)_n-$	C-C	ν

ν stretching, δ deformation

However, the most important spectral features appear in the fingerprint region. Two bands near 1,121 and 1,098 cm^{-1} show interesting spectral features. The absorbance intensity in the vicinity of 1,121 cm^{-1} shows a positive correlation with the amount of oleic acid, while the intensity near 1,098 cm^{-1} is correlated with the amount of linoleic acid (Aparicio and Baeten 1997). In addition, the peak centered at 913 cm^{-1} is not present (or is very weak) in high oleic sunflower and olive oil, while it is more intense in samples rich in polyunsaturated fatty acids. Table 10.6 shows the wavenumbers with a coefficient of correlation between the absorption

Table 10.8 Relevant Raman shifts (cm^{-1}) of several lipids and bands that are correlated with some chemical indices (R>0.90)

	Spectral region		
Lipids	= C-H stretching	C=C stretching	C-H bending
Methyl oleate (*cis* C18:1)	3,006	1,654	1,439, 1,267
Methyl elaidate (*trans* C18:1)	2,995	1,667	1,439
Methyl linoleate (*cis* C18:2)	3,011	1,657	1,440, 1,265
Methyl linolenate (*cis* C18:3)	3,013	1,657	1,441, 1,266
MUFA	2,890, 2,874[a], 2,845		
PUFA	3,021, 2,922, 2,884[a], 2,870, 2,855[a]	1,667, 1,642	1,256
IV	3,007, 2,991, 2,911, 2,882[a], 2,855[a]	1,657, 1,646	1,268

UFA unsaturated fatty acids, *MUFA* monounsaturated fatty acids, *PUFA* polyunsaturated fatty acids, *SFA* saturated fatty acids, *IV* iodine value
[a]negative correlation coefficient

intensities and different chemical indices higher than 0.90. The region near 3,010–2,950 cm^{-1} and the fingerprint region (1,500–700 cm^{-1}) show the highest correlation with the different indices in relation to the degree of unsaturation of the samples.

10.5.3 Raman Spectra

The spectra of edible fats and oils obtained by FT-Raman spectrometers contain well-resolved bands with various scattering intensities and shapes. The spectra show good signal-to-noise ratios and contain information from different vibrational bands (stretching and bending) of various chemical groups. Raman scattering arises from the change in the polarizability or shape of the electron distribution in the molecule as it vibrates, while, in contrast, IR absorption requires a change in the intrinsic dipole moment with the molecular vibration (Grasseli and Bulkin 1991). Hence, polar groups (such as C=O and O-H) have strong MIR absorption bands, whereas nonpolar groups (such as C=C) show intense Raman scattered bands. Because the main feature of unsaturated fatty acids is their content of double bonds and their configuration (*cis* or *trans*), FT-Raman spectra are of great value in the study of lipids. Raman spectroscopy has been used in the determination of the total amount of unsaturation (iodine value) and of the *cis/trans* isomer content of edible oils (Bailey and Horvat 1972; Sadeghi-Jorabchi et al. 1990, 1991). Figure 10.15 and Table 10.7 display respectively the FT-Raman spectrum and the assignment of the most noteworthy bands of a virgin olive oil.

Bailey and Horvat (1972) studied the spectral features in the area of 1,660 cm^{-1} (C=C stretching vibration) of triolein, trielaidin, trilinolein, and trilinolenin. In this region, *trans* isomers had a peak centered near 1,670 cm^{-1}, while *cis* isomers showed a peak in the vicinity of 1,660 cm^{-1}. Later on, Sadeghi-Jorabchi et al. (1991) studied and underlined other characteristics of pure methyl esters in their work on the quantification of *cis* and *trans* content by FT-Raman spectroscopy. They showed the particular features of fatty acids near 3,010 cm^{-1} (=C-H

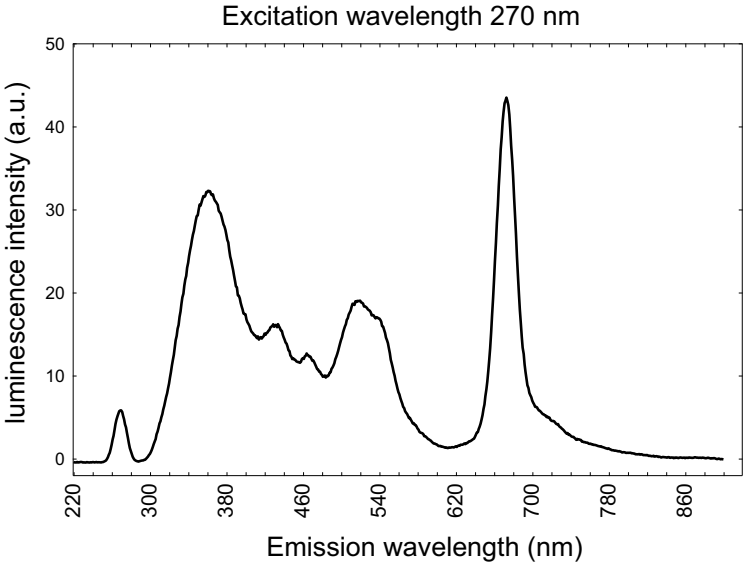

Fig. 10.16 Fluorescence spectra of a virgin olive oil

stretching vibration) and 1,270 cm^{-1}(=C-H bending vibration). In the area of 3,010 cm^{-1} a shift to a higher frequency and an increase in the scattering intensities occurs as the degree of unsaturation rises. Similar observations were reported at 1,660 and 1,270 cm^{-1}. Table 10.8 shows the main characteristics of various methyl esters.

The region near 3,010 cm^{-1} is particularly affected by the major fatty acid components (Baeten et al. 1998). In fact, samples relatively rich in polyunsaturated fatty acids (e.g., corn, sunflower, and sesame oils) had a more intense scattering band and a higher frequency maximum than samples rich in monounsaturated fatty acids (e.g., olive oil). This band is also important in the authentication of olive oil (Baeten et al. 1996). The usefulness of Raman shifts in the range 2,880–2,840 cm^{-1} (C-H stretching vibration of CH_2 and CH_3) for varietal discrimination has also been noted (Aparicio and Baeten 1998). In this region, samples rich in polyunsaturated fatty acids (e.g., rapeseed, sunflower, and walnut oils) have weaker scattering intensities than those that have a high content of monounsaturated fatty acids (e.g., olive oil).

The region of 1,660 and 1,265 cm^{-1} is also characteristic of the fatty acid profile of the fat or oil variety studied. Samples rich in polyunsaturated fatty acids such as walnut, sunflower, corn, and sesame oils have a maximum near 1,657 cm^{-1}, while olive and high oleic sunflower show a maximum near 1,655 cm^{-1}. The intensity at these Raman shifts rises with the degree of unsaturation. Near 1,259 cm^{-1}, the scattering intensities increase as the degree of unsaturation decreases. The fingerprint region (1,100–700 cm^{-1}) of pure methyl esters and of different oil varieties also have information (Sadeghi-Jorabchi et al. 1991). However, the poor signal-to-noise ratio

Table 10.9 Emission wavelength associated with fluorophores present in olive oil

Fluorescent compounds	λ_{em} (nm)	Reference
Pigment (chlorophylls and pheophytins)	692–765	Sayago et al. (2007)
α-, β-, and γ-tocopherols, phenols	275–400	Dupuy et al. (2005)
Chlorophyll a and b, pheophytin a and b	600–700	
Oxidized products from vitamin E	400–600	
Tocopherols and tocotrienols	300–350	Sikorska et al. (2005)
Chlorophylls and pheophytins	660–700	
Oxidized product	400	
Phenols	300–390	Zandomeneghi et al. (2005)
Chlorophylls and derivatives	640–800	
Tocopherols	328	Giungato et al. (2004)
Chlorophyll a	669	
Parinaric acid isomerization	406	
Vitamin E (oxidized products)	440, 475, 525	Guimet et al. (2004)
Chlorophylls	650 y 700	
Chlorophyll a	669	Galeano et al. (2003)
Chlorophyll b	653	
Pheophytin a	671	
Pheophytin b	658	
Hydroxyl radical	452,3	Tai et al. (2002)
K232 y K270	440–445	Kyriakidis and Skarkalis (2000)
Vitamin E derivatives	525	
Chlorophylls	681	

at these frequencies does not allow, at the moment, evaluation of the information. Table 10.8 regroups the wavenumbers showing a maximum coefficient of correlation between the absorption intensities and different chemical indices.

10.5.4 Fluorescence Spectra

Vegetable oils are commonly analyzed by fluorescence spectroscopy untreated or diluted at 1 % in hexano v/v. In particular, Fig. 10.16 displays the fluorescence spectrum of a virgin olive oil in its native form (nondiluted). The bands observed in this spectrum have been related to species that are shown in Table 10.9. In this table also appears the emission wavelength of these fluorophores. The spectral profile and the intensities of these bands dramatically vary with the oxidation degree of the samples, as was shown in Fig. 10.3. The bands of some fluorescent compounds, such as chlorophylls, are more intense than other fluorescent species, although the intensity greatly depends on the excitation wavelength. The magnitude of this peak with respect to others may cause problems when handling the whole data set. This

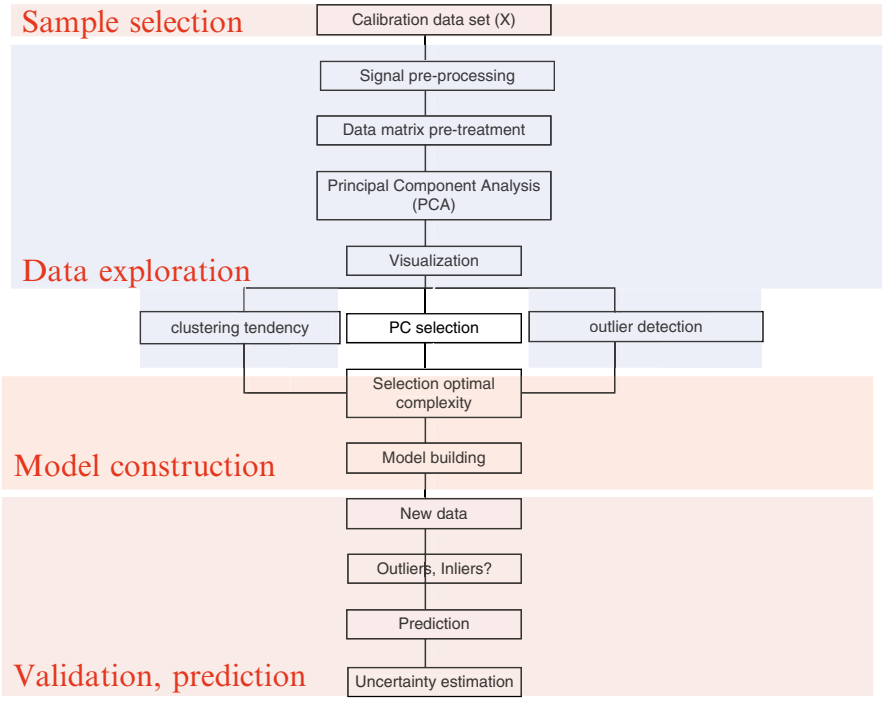

Fig. 10.17 Flow diagram showing principal steps involved in a spectral data treatment

problem can be avoided by studying narrower ranges of wavelengths instead of processing the information of the entire emission spectra.

10.6 Data Treatment

The main analytical problem with spectroscopic data is to extract the information in such a way that it can be used in quantitative analysis. IR and Raman spectra are usually the mean of various coadded spectra (normally between 100 and 200). The collection of a high number of coadded spectra is allowed by the rapidity of the acquisition of a single coadded spectrum in an FT instrument (around a few seconds). The spectra displayed throughout the present chapter are coadded spectra. These spectra are a rich source of multivariate data (more than 700 data points) where each frequency represents a variable. Various strategies have been proposed to investigate the spectral data set and to isolate areas, patterns, or latent variables correlated with the information concerned.

Figure 10.17 summarizes the classical steps for building a mathematical model (i.e., a quantitative or discriminant equation). The steps are the pretreatment of data,

outlier detection, calibration, and validation procedures including chemical, internal, and external validation.

The following sections briefly describe the data treatments and their respective objectives. For a thorough presentation of the ideas in this section, the reader may refer to Tabachnick and Fidell (1983), Williams and Norris (2001), and Martens and Naes (1989).

10.6.1 Pretreatment of Data

The signal obtained from a spectrometer contains information together with random noise. Noise can cause systematic errors in later predictions through the estimated calibration parameters. Thus, reducing noise or, in other words, improving the ratio of signal to noise is still an advantage.

Various pretreatments of data are available for different objectives, such as, for example, to improve the spectral quality (e.g., signal-to-noise ratio), to reduce the influence of external variation (e.g., variation produced by the sample-handling method), or to resolve the complexity of overlapping peaks (e.g., the combination bands or the fingerprint region of MIR spectroscopy). All depend on the objective sought, the technique investigated, the instrument and sample accessory used, the sample (neat or solution) studied, the type of mathematical model to be built, or the researcher's preferences.

Various algorithms are available to perform smoothing that basically concern how to reduce high-frequency ripple noise and, whenever possible, low-frequency noise. Thus, conceptually speaking, smoothing is simply a filtering process. From the large panoply of algorithms developed for electronic analog and computer systems from the 1960s to today, algorithms are available in the smoothing routines of the software packages developed for IR and Raman spectrometers. These routines usually contain algorithms such as moving average filters (Rabiner and Gold 1975), the least-squares polynomial smoothing developed by Savitsky and Golay (1964), and the classical Fourier smoothing methodology (Williams and Norris 2001; Martens and Naes 1989), among others. The running mean algorithm simply replaces the value at each point by the mean of the values in a wavelength (or wavenumber) interval surrounding it. The interval is centered at the given point, resulting in an odd number of data points per mean (Williams and Norris 2001). The Savitsky–Golay algorithm, the most familiar method of smoothing in analytical chemistry, is an indirect filter that fits the spectrum inside a wavelength (or wavenumber) interval with a polynomial by least-squares method. The parameters are the degree of the polynomial and the number of points to fit (Savitsky and Golay 1964). Fourier analysis makes an orthogonal transformation of the spectrum into a sum of sine and cosine spectral contributions (Aparicio et al. 1977) that allows certain frequencies to be kept (usually low frequencies) and removes those undesired frequencies that do contribute to noise (often the high-frequency ripple). The inverse FT is ultimately used for regenerating the spectrum.

Derivatives allow some compensation for the problems associated with overlapping peaks and baseline variations. Analysts generally use the first and second derivatives. This mathematical treatment calculates the tangent at each point of the raw spectral data. Each inflection point of the raw spectrum corresponds to a relative minimum or maximum of the first derivative spectrum while all maxima and minima on the raw spectrum are zero in the first derivative spectrum. The second derivative is advantageous for the resolution of overlapping peaks. Each minimum of the second derivative spectrum corresponds to a maximum of the raw spectrum, and obviously identical comments can be made regarding successive even derivatives (Williams and Norris 2001).

Normalization means changing a group of spectra so that unwanted sources of variability are suppressed. This helps the graphical understanding of the spectra and can reduce the complexity of the subsequent data treatment necessary to develop a calibration from spectroscopic data. The simplest example of this treatment is the subtraction of the spectral value at a single wavelength or wavenumber (the so-called reference wavelength or wavenumber) from all the spectral values; the result is a set of spectra with zero value at the reference wavelength or wavenumber. Normalization by closure is an alternative. This normalization consists in dividing the signal instrument responses at each wavelength or wavenumber by their sum (or mean) in each spectrum. Martens and Naes (1989) suggest this procedure when there is no variable that dominates the total sum of original instrument responses, but always after a graphical inspection of the ratios between some estimated values for independent variables.

Outliers are abnormal, erroneous, or irrelevant observations that can greatly influence mathematical model construction. A number of phenomena such as operator mistakes, noise spikes, instrument drifts, and inconsistent sample-handling position can affect a spectroscopic analysis (Williams and Antoniszyn 1987). Thus, both objects (cases) and variables can behave as outliers, and they are unavoidable in almost all statistical studies. They can only be removed or corrected. During calibration it is important to have them under control as they could decrease the prediction ability of the estimated calibration coefficients. The cross-validation curve can give clues about the presence of outliers in the calibration set, e.g., irregular deviations of the fitted curve of MSE versus the number of PLS factors (Martens and Naes 1989), although almost all multivariate statistical procedures have algorithms for outlier detection (Tabachnick and Fidell 1983). Other algorithms are based on leverage (a Mahalanobis distance that measures the position of independent variables relative to the rest) and residuals (difference between predicted and observed values in regression). Leverage is outlier sensitive, and a high leverage observation in a regression process means that the calibration set contains outliers. A plot of residuals (residuals against wavelength numbers) gives more than graphical information because an observation with large residuals indicates the presence of abnormal information (Cook and Weisberg 1982).

During prediction it is almost compulsory to have methods for detecting abnormalities in order to increase the certainty of the predicted results. The detection of these possibly abnormal observations can be based on data information such as the residual value and the prediction leverage (Martens and Naes 1989) or more classical methods based on the Mahalanobis distances (De Maesschalck et al. 2000) and on potential functions (Jouan-Rimbaud et al. 1999). Robust methods (Geurts et al. 1990) can also be applied such as resampling by the half-means (RHM) or the smallest half-volume method (SHV) (Egan and Morgan 1998; Pell 2000). However, most of these multivariate outlier detection techniques are often difficult to understand for nonspecialists and are not an easy matter due to the masking and swamping effects. The masking effect occurs when one outlier masks a second outlier. In this case, the second outlier can be considered an outlier only by itself, not in the presence of the first outlier. In the swamping effect, one outlier swamps a second observation because the latter can be considered an outlier only in the presence of the first one (Ben-Gal 2005). Most analytical chemists want to spend as little time as possible looking at the large variety of diagnostics for outlier detection. In consequence, simple methods are needed. For this reason, complete protocols for outlier detection have been developed with the maximum information that can be extracted from the data (Høy et al. 1998; Fernández Pierna et al. 2002). These protocols include not only the determination of classical measurements as Mahalanobis distance or the leverage value, but also the calculation of the uncertainty present in the outputs of the multivariate model, which is calculated as a function of the different sources of uncertainty present in the model (Fernández Pierna et al. 2003).

After analysis of the internal and external variables that can affect the mathematical model, the pretreatment of data should finish with a study of the repeatability and reproducibility of the method. The main element of repeatability is the standard deviation of a successive collection of spectra of the same sample under the most realistic experimental conditions. The repeatability study should include not only all the steps included in the data collection procedure (washing of the sample holder, sample removal, spectral acquisition), but also a study of the variability observed on different days. Reproducibility would imply a collaborative study about the comparison of spectral results of selected samples by diverse instruments at different laboratories. The results of the repeatability and reproducibility studies firmly determine the number of replicates of each case (sample) of the calibration and validation sets and the regions of the spectra that can be used in calibration.

10.6.2 Mathematical Model Construction

The purpose of IR and Raman instruments is to determine the concentration of chemical variables, such as *trans* content (i.e., quantitative analysis), or the assessment of

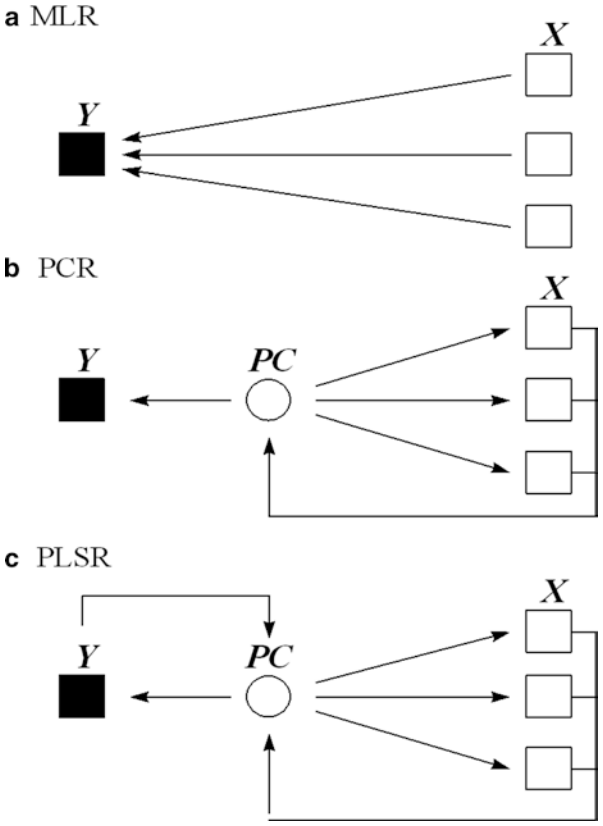

Fig. 10.18 Schematic presentation of (**a**) multivariate regression analysis (*MLR*), (**b**) principal component regression (*PCR*), and (**c**) partial least-squares regression (*PLSR*)

qualitative issues, such as authenticity or characterization (i.e., qualitative analysis). But to do this, the instrument must be calibrated for converting the IR or Raman optical signal to the desired quantitative or qualitative measurement. A model needs two processes, the calibration, or model design, and the validation, or model verification.

Calibration is usually carried out with chemical parameters (i.e., iodine value) quantified by nonspectroscopic techniques, e.g., chromatography. The dependent variable (e.g., iodine value) is then qualified as a direct measurement, while the independent variable (the spectrum) is described as an indirect measurement. However, it is the spectroscopic technique that responds directly to the problem description. For example, peptide bonds in proteins are directly represented in the spectrum, whereas the so-called direct method Kjeldahl analysis for proteins involves the measurement of total nitrogen, which requires several reaction steps and the application of a conversion factor to amine and protein measurement (Scotter 1997).

10.6.2.1 Calibration in Quantitative Analysis

Calibration means a formula (linear or nonlinear) establishing a relationship between the variation of the spectral data (independent variable) and the chemical reference data (dependent variable). The calibration is in fact a regression process with a strict pretreatment of data and rigorous analysis of the results.

Since two steps are necessary to achieve a mathematical model construction (calibration and validation), two sample sets are necessary, i.e., a set of *N* samples that would be used to construct the equation (calibration set) and a set of *M* samples that would allow studying the precision and the reliability of the equation (validation set). The number of samples in the validation set should be at least half of the calibration set. Moreover, the mean and the standard deviation of the two sample sets must be as close as possible, and the validation set must also be a subset of the calibration set covering the whole range of values. To assure these conditions and to have two homogeneous data sets, i.e., which should cover the experimental region uniformly, various methods have been developed and are described in the literature. The most common technique is the duplex method (Snee 1977), which is a modification of the Kennard and Stone technique (Kennard and Stone 1969). In this method, a sequential procedure is applied in order to split the data into two subsets. The method starts by selecting the two points that are furthest from each other and puts them both in a first set (training). Then, the next two points that are furthest from each other are put in a second set (testing), and the procedure is continued by alternately placing pairs of points in the first or second set.

Various calibration (or regression) procedures exist, with multiple linear regression (MLR), principal component regression (PCR), and PLS being the most commonly used in spectroscopy. Figure 10.18 shows a schematic design of these statistical procedures where the matrix Y_{ij} (or **y**) represents the values of the *j*-dependent variables (usually chemical analyses) of *N* ($i = 1 \ldots N$) calibration samples, while matrix X_{iw} (or **X**) represents the values of *w*-independent variables (spectral wavelengths or wavenumbers) of these *N* calibration samples. The simple regression equation can be written, in matrix convention, $\mathbf{y} = \mathbf{Xb} + \mathbf{f}$, while the objective of the calibration by least squares is to minimize the length $\mathbf{f} = \mathbf{y}\text{-}\mathbf{Xb}$ whose solution is equal to *Estimator*-$\mathbf{b} = (\mathbf{X}'\mathbf{X})^{-1}\ \mathbf{X}^{-1}\mathbf{y}$, where $\mathbf{X}'$ is the transpose matrix **X** and $\mathbf{X}^{-1}$ is the inverted matrix **X**.

The explanation of a dependent variable (e.g., iodine value) by only one wavenumber is rather difficult, and hence calibration needs to combine more than one wavenumber; this is multivariate calibration. Traditional MLR and stepwise multiple linear regression (SMLR) are expressed as

$$y = b_0 + \sum X_i b_i + \delta,$$

where *y* is the dependent variable, or analytical reference, $X_{i(i=1,n)}$ (the independent variables) are the spectral data (transformed or not) at the respective *n* wavelengths or *n* wavenumbers, and b_i ($i = 0,1,\ldots,N$) are the regression coefficients. To achieve higher regression values, the analyst might be tempted to increase the number of

spectral data in calibration; however, it is judicious to limit the number according to the sample number. Tabachnick and Fidell (1983) suggest that the number of samples should be ten times the number of independent variables. Anyway the MLR predictor has a deficient performance when there is collinearity in **X**, while SMLR gives a better prediction when an F-test is used for selecting variables because this algorithm enables removal of those X_i-variables that are most nonlinear in their response (Tabachnick and Fidell 1983).

Partial least-squares regression (PLSR) was designed to give a plausible solution to those studies where there are many collinear variables and a small calibration set, that is to say, where the number of variables is greater than cases (spectra), although some pitfalls have been described (Defernez and Kemsley 1996). PLSR can be applied for one single *y*-variable and several *y*-variables. In general PLSR-1 is more complex than PCR or PLSR-2 than canonical correlation based on simultaneous PCA of **X** and **Y** matrices. Martens and Naes (1989) state that calibration methods based on PLS regression can give a good understanding of the calibration data and a good approximation of many types of nonlinearities. Other alternative is ridge regression (Pfaffenberger and Dielman 1990), although it has not been widely used in spectroscopy despite the fact that it can be superior to PCR.

One of the most common applications of PCA is in those studies where X_i-variables are expected to be collinear. This is the case with spectral analysis (Cowe et al. 1985a, b), and PCA is able to express the main information in the variables of the raw calibration set by a lower number of variables, so-called principal components (Chap. 12). Once the analyst has decided how many principal components are necessary for retaining the essential information in **X** (i.e., applying cross validation), the rest of the process is similar to MLR, although the application of SMLR to PCA is strongly advised (Aparicio et al. 1992). At any rate, the analyst should select the best spectral data instead of the whole spectrum as the latter can contain large amounts of noise or superfluous information.

The described regression procedures assume that the relationship between the independent variables and the dependent variable is linear in nature. However, the nonlinear estimation leaves it up to the analyst to specify the nature of the relationship; for example, you may specify the dependent variable to be a logarithmic function of the independent variables, an exponential function, a function of some complex ratio of independent measures, etc. There are many noncategorical nonlinear estimations such as the quasi-Newton method (O'Neill 1971), piecewise nonlinear regression, Hooke–Jeeves method (Hooke and Jeeves 1961), simplex procedure (Fletcher and Reeves 1964), Hessian method, and others. Where all these other methods fail, the Rosenbrock pattern search method often succeeds. This method rotates the parameter space and aligns one axis with a ridge while all other axes remain orthogonal to this axis. If the loss function is unimodal and has detectable ridges pointing toward the minimum of the function, then this method will proceed with accuracy toward the minimum of the function. However, if all variables of interest are categorical in nature, or can be converted into categorical variables, the correspondence analysis module should also be considered.

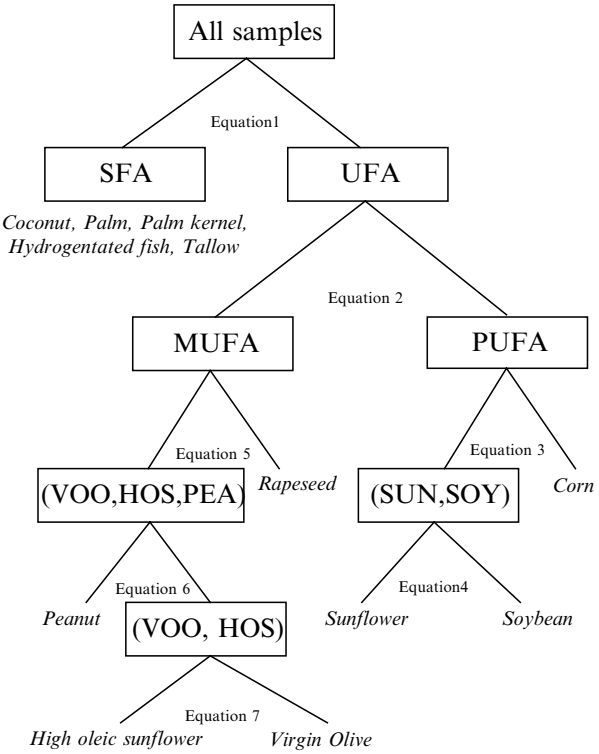

Fig. 10.19 Discrimination tree constructed using near-infrared and Raman spectral data. Legend: *SFA* samples rich in saturated fatty acids, *UFA* samples rich in unsaturated fatty acids, *MUFA* samples rich in monounsaturated fatty acids, *PUFA* samples rich in polyunsaturated fatty acids, *VOO* virgin olive oil, *HOS* high oleic sunflower, *PEA* peanut, *SUN* sunflower, *SOY* soybean

It is important to note that sometimes data are nonlinear. Deletion or appropriate weighting of nonlinear variables at the beginning of an analysis can decrease the nonlinearity problems. Also, in some cases an appropriate signal preprocessing can correct for the nonlinearity. These approaches can perhaps give better predictive ability than linear models with original variables or less complex models for the same predictive ability; however, alternatively, one may decide to adopt nonlinear models such as neural networks, support vector machines (SVM), or local regression approaches (De Maesschalck et al. 1999).

10.6.2.2 Qualitative Analysis: Classification Protocols

To construct a mathematical model for olive oil characterization or authentication, it is important to establish an intelligible, reproducible, valid, and predictive approach. Unfortunately, few authors propose a complete procedure to extract and use the information contained in IR or Raman spectra. The following sections are based on the results obtained with two protocols (Lai et al. 1994).

The first step of these two approaches is identical and concerns the division of the sample set into two subsets. As mentioned previously, the first subset

(calibration set) is used to construct the discrimination equation, while the second subset (validation set) permits the validation of the established model. The sample set studied must include all possible combinations of variables and the variation in all directions should be as large as possible but limited to the direction of interest (Naes and Isakson 1989).

In the procedure suggested by Lai et al. (1994), PCA is used because it constitutes an efficient data reduction method. As mentioned previously, a spectrum contains several hundred variables. But a multivariate statistical analysis requires that the case (sample) number exceed the variable number, and as a consequence, a reduction in the spectral variable number is necessary. Furthermore, the PCA procedure allows the removal of the apparent redundancy of the variables by transforming the original data into a set of principal component scores. When this is done, a rearrangement of the data takes place and the first few PC scores are sufficient to describe the information contained in the original variables. This procedure allows for data set simplification and the visualization of relationships within the data. After applying PCA, Lai et al. (1994) used discriminant analysis to construct a mathematical model on the basis of the scores. The squared Mahalanobis distances (SMD) are used to classify each case (sample) inside the predetermined groups. Later, the SMD from the established group means are calculated for each validation spectrum's PC scores and the new samples will be assigned to the nearest group mean. The percentage of correct classifications corresponds to the samples assigned to the correct group (i.e., species).

The approach presented by Aparicio and Baeten (1998) uses stepwise linear discriminant analysis (SLDA) to select frequencies and construct the mathematical models. SLDA is first applied to each part of the spectrum in such a way that the more relevant frequencies from each region are selected. After that, the SLDA procedure is applied to all the preselected variables and the discriminating equations are established on the basis of Mahalanobis distance and F-test (Tabachnick and Fidell 1983). The ellipses of the 95 % confidence region are calculated for each predetermined group during the calibration step (Aparicio and Baeten 1997). These ellipses allow an interpretation beyond the simple location of a validation sample and the calculation of the percentage of samples correctly classified during the validation procedure (Aparicio and Morales 1995). An alternative to these procedures could be to apply the Fisher test for removing variables without precise information and then apply PCA on the selected variables. The model can be used in an arborescent structure for distinguishing different types of fats and oils (Fig. 10.19).

Also, classical chemometric methods such as partial least squares discriminant analysis (PLSDA) (Martens and Naes 1989), and artificial neural networks (ANN) (Despagne and Massart 1998) are well-known and proven techniques for both qualitative and quantitative analysis of multivariate data. In the case of qualitative analysis, the SVM technique (Vapnik 2000) has been recently proposed and widely used in the literature (Burges 1998; Belousov et al. 2002; Fernández Pierna et al. 2004). The choice of SVM as classification method is justified by the great performance of these methods in all studies, which is mainly due to the uniqueness of the SVM solution for the problems of pattern recognition.

10.6.3 Validation Procedures

Analysts should pay attention to the validation procedures, which include the chemical, internal, and external validations (Fig. 10.17). Chemical validation is the interpretation and the elucidation (band assignment) of the frequencies used in the mathematical model. All selected spectral data (frequencies) should have a chemical or physical explanation in order to avoid regressions obtained by chance. To do this step successfully, the study of the spectral features (position and intensity of the bands) of pure chemical compounds and the correlation at each frequency between the intensities and chemical properties (e.g., determined by gas chromatography) is necessary.

Internal and external validations consist in the study of the efficiency and power of the mathematical models constructed. Internal validation is done with the samples involved in the construction of the equation (calibration step). Cross validation is a particular internal validation method (Martens and Naes 1989), although there are others such as leverage correction or Mallows *Cp* statistic (Chap. 12). An external validation is made by the observation of the quantification (quantitative analysis) or the classification (qualitative analysis) of new samples not used in the calibration procedure. The number and characteristics of these samples have been clearly established (Aparicio et al. 1992).

In order to perform a correct validation and to indicate the performance of the results, different standard expressions taken from basic statistics are applied. However, multivariate models are inherently complex, and as a result, theoretical advances with respect to the corresponding error analysis are relatively slow. For this reason, developing approximate expressions for sample-specific standard error of prediction when applying a multivariate model, mainly PLS, has received considerable attention in the chemometric-related literature in recent years (Faber 2000; Faber and Bro 2002). This calculation of uncertainty consists in the study of the uncertainty present in the outputs of the model. In most cases, this uncertainty is calculated as a function of the various sources of uncertainty present in the model (Fernández Pierna et al. 2003).

10.7 Potential of Infrared and Raman Spectroscopy

The potential offered by NIR, MIR, and Raman spectroscopy in the determination of various chemical compounds and chemical indices has been described, with more or less success, by various authors (Williams and Norris 2001; van de Voort 1994; Li-Chan 1996; Guillén and Cabo 1997). The following section briefly describes the methods used with olive oil, whereas their application in characterization is described in Chap. 12.

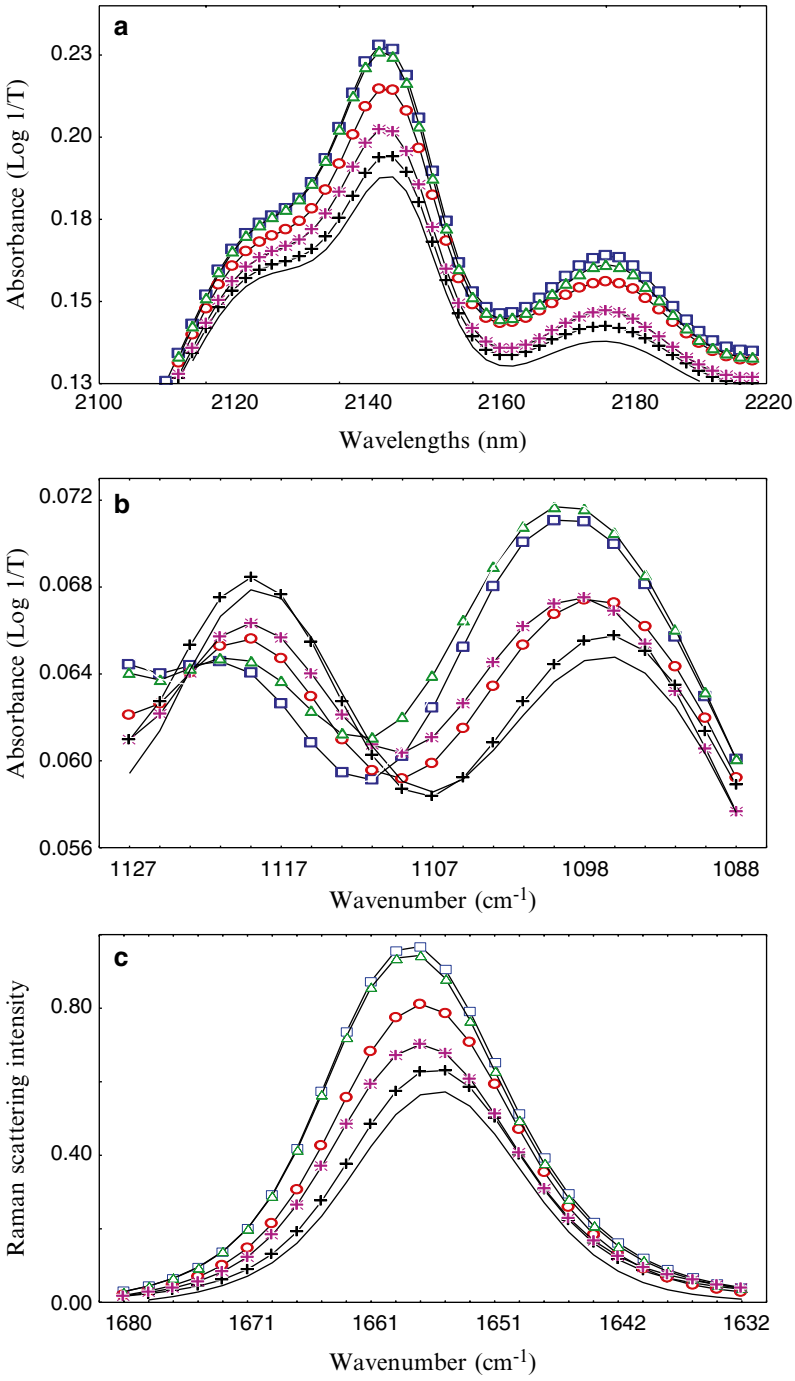

Fig. 10.20 Spectral regions of (**a**) near-infrared, (**b**) FT-mid-infrared, and (**c**) FT-raman spectra of the following edible oils: (⊟) sunflower oil, (-○-) rapeseed oil, (✳) peanut oil, (△) soybean oil, (✚) high oleic sunflower oil, and (—) virgin olive oil

10.7.1 Determination of Unsaturation Degree: Iodine Value

As was mentioned earlier, NIR, MIR, and Raman spectrum profiles are strongly influenced by the content and type of unsaturated groups. Figure 10.20 presents a spectral region of various edible oils and fats for each technique investigated. The regions shown are, respectively, the region 2,100–2,200 nm (=C-H vibration) of NIR spectra, the region 1,130–1,080 cm^{-1} (C-C and C-O-C vibration) of MIR spectra, and the region 1,680–1,650 cm^{-1} (C=C vibration) of Raman spectra.

Fenton and Crisler (1959) published a study showing the potential of NIR spectroscopy. They developed, using a series of chemical products, a rapid and reliable technique for the determination of the iodine value. The calibration equation was constructed with the information contained in the region 2,100–2,200 nm of the NIR spectrum. Some years earlier, Sinclair et al. (1952) had described the linear relationship between the number of *cis* double bonds of unsaturated fatty acid methyl esters and the ratio between the absorbance at 2,920 cm^{-1} (>CH_2 vibration) and the difference between the absorbances at 2,920 and 3,020 cm^{-1} (=C-H vibration). This study was later confirmed by the results achieved by other authors who proposed MIR spectroscopy as a technique to determine the degree of unsaturation (Chapman 1965). Later, Arnold and Hartung (1971), using the ratio of absorbances at 3,030 cm^{-1} (=C-H vibration) and 2,857 cm^{-1} (>CH2 vibration), showed the potential of a MIR instrument equipped with a transmission cell for iodine value determinations in fats and oils. Using the absorbance of wavenumbers from the same region (3,010 and 2,854 cm^{-1}), Afran and Newbery (1991) demonstrated the potential of an FT-MIR instrument coupled with an ATR accessory. The absorption intensities at 3,007 cm^{-1} (=C-H vibration) (Muniategui et al. 1992) and at 1,658 cm^{-1} (C=C vibration) (Bernard and Sims 1980) were also used to determine the total degree of unsaturation.

A FT-MIR/ATR instrument, together with a PLS procedure, was used by van de Voort et al. (1992) for determining the iodine value using TAGs as dependent variables. Spectral information from regions 3,200–2,600 cm^{-1} and 1,600–1,000 cm^{-1} was successfully used. Bailey and Horvat (1972) showed the high correlation between the iodine value and the ratio of the scattering intensities in the regions 1,691–1,626 cm^{-1} (C=C vibration) and 1,478–1,420 cm^{-1} (>CH_2 vibration) using Raman spectroscopy. Later, a Raman spectrometer equipped with a NIR excitation and interferometry technology was used by Sadeghi-Jorabchi et al. (1990) to study the possibilities offered by the new generation of such instruments in the determination of iodine value of oils and margarines. The quantitative program designed in this study used information from the scattering bands centered at 1,656 cm^{-1} (=C-H vibration) and at 1,444 cm^{-1}. The peaks in the vicinity of 3,010 cm^{-1} (=C-H stretching vibration) and 1,270 cm^{-1} (=C-H bending vibration) also showed a high correlation with the iodine value (Sadeghi-Jorabchi et al. 1991; Baeten et al. 1998).

10.7.2 Determination of Trans *and* Cis *Content*

Infrared methods for determining the *trans* isomer content of oils and fats are standardized (IUPAC 1992; AOCS 1988). These methods are based on the absorption band at 967 cm^{-1} (*trans* CH=CH vibration). However, Lanser and Emken (1988), using the peak area of the *trans* absorbance band at 966 cm^{-1}, estimated the *trans* unsaturation, which agreed with the results obtained by gas chromatography. Belton et al. (1988) used FT-MIR combined with ATR to develop a procedure for the estimation of isolated *trans* double bonds in oils and fats. Sleeter and Matlock (1989) developed a FT-MIR procedure for measuring the *trans* content of oils in a 100-μm KBr cell. Ulberth and Haider (1992) used *trans*-free methylated soybean oil mixed with methyl elaidate in combination with a FT-MIR spectral subtraction technique and PLS to assess low concentrations of isolated *trans* double bonds in hydrogenated fats such as margarine and shortenings. Then, van de Voort et al. (1995) designed a generalized, industrial sample-holder accessory for handling both fats and oils. It was incorporated into a FT-MIR spectrometer, and a method using PLS calibration was developed to determine the *cis* and *trans* contents of neat samples. Mossoba et al. (1996) also used attenuated total reflection spectroscopy to calculate the total *trans* content of hydrogenated oils by the information of the spectral region between 990 and 945 cm^{-1}.

Using Raman spectroscopy, Bailey and Horvat (1972) also determined the *cis/trans* isomer content of edible vegetable oils by measuring the intensities of C=C stretching fundamentals near 1,657 and 1,670 cm^{-1} that are associated with *cis* and *trans* configurations, respectively. As seen earlier, the use of FT-Raman spectroscopy has proved to be successful in the determination of total unsaturation of oils and margarines (Sadeghi-Jorabchi et al. 1990). Furthermore, Sadeghi-Jorabchi et al. (1991) have also used the FT-Raman scattering information from bands centered near 1,670, 1,656, and 1,444 cm^{-1} to estimate various levels of *cis* and *trans* isomers mixtures. A similar approach was used by Ozaki et al. (1992) to estimate the level of unsaturation of a wide range of fat-containing foodstuffs.

10.7.3 Determination of Saponification Number, Solid Fat Index, and Free Fatty Acids

Using the information obtained from a FT-MIR spectrometer equipped with an ATR accessory and the PLS methodology, van de Voort et al. (1992) proposed a method to determine the saponification number. They used the information contained in two MIR regions: 3,200–2,600 cm^{-1} and 1,850–1,000 cm^{-1}. Van de Voort et al. (1996) also showed the potential of MIR spectroscopy in the determination of the solid fat index. The calibration was done with selected parts of the spectrum: 3,015–3,005 cm^{-1}, 3,000–2,850 cm^{-1}, 1,750–1,740 cm^{-1}, 1,550–1,050 cm^{-1}, 980–960 cm^{-1}, and 750–730 cm^{-1} by a FT-MIR spectrometer equipped with a flow transmission

cell and PLS. Lanser et al. (1991) used peaks near 1,745 and 1,711 cm^{-1} to construct a model allowing the determination of the free fatty acid content in crude oils. The C=O carbonyl group of esters is present near 1,746 cm^{-1}, while the carboxylic group of free fatty acids has its characteristic peak at 1,711 cm^{-1}. Later, an FT-MIR instrument and ATR accessory were successfully used to determine the free fatty acid content in oils and fats (Ismail et al. 1993).

10.7.4 Monitoring the Oxidative Process, Measuring the Peroxide and Anisidine Values

The potential of FT-MIR instruments for the study of the complex changes that take place in a sample involved in an oxidation process has also been investigated (van de Voort et al. 1994a). The authors used oils oxidized under various conditions and recorded their MIR spectral changes. They identified the most noteworthy bands associated with common oxidation end products such as, for example, hexanal, decadienal, (E)-butyl hydroxide, demonstrating the usefulness of FT-MIR spectroscopy to detect oxidative changes.

A method based on FT-MIR spectroscopy was also proposed for the simultaneous monitoring of aldehyde formation and the determination of the anisidine value in thermally stressed oils (Dubois et al. 1996). The authors added aldehydes to an oil sample and thus built a calibration model by PLS.

10.8 Potential of Fluorescence Spectroscopy

Fluorescence spectroscopy is a rapid analytical technique with high sensitivity to determine the overall presence of series of compounds. The use of fluorescence to analyze olive oils was first proposed in 1925 by Frehse, who studied the possibility of detecting the presence of refined olive oil in virgin olive oil by examining the oils under a quartz lamp with a Wood filter; another early work showed good prospects for characterization of edible oils through fluorimetry techniques (Wolfbeis and Leiner 1984). However, this highly sensitive technique has been largely ignored for the characterization of edible oils. Only recently has progress been achieved in spectrofluorometers and several fluorescence techniques that have been introduced to facilitate the analysis of complex food. Thus, fluorescence spectroscopy has considerable potential to characterize virgin olive oils because of the large variety of fluorescent compounds (chlorophylls, pheophytins, tocopherols, vitamin E, and oxidized compounds) present in them (Sikorska et al. 2004; Guimet et al. 2004; Galano et al. 2003). On the other hand, there are remarkable differences between the fluorescence spectra of virgin olive oil and the other edible oils (Sikorska et al. 2005), which encourages the use of this technique for authentication purposes. The various categories of virgin olive oil also show particular emission spectra (Nicoletti 1990).

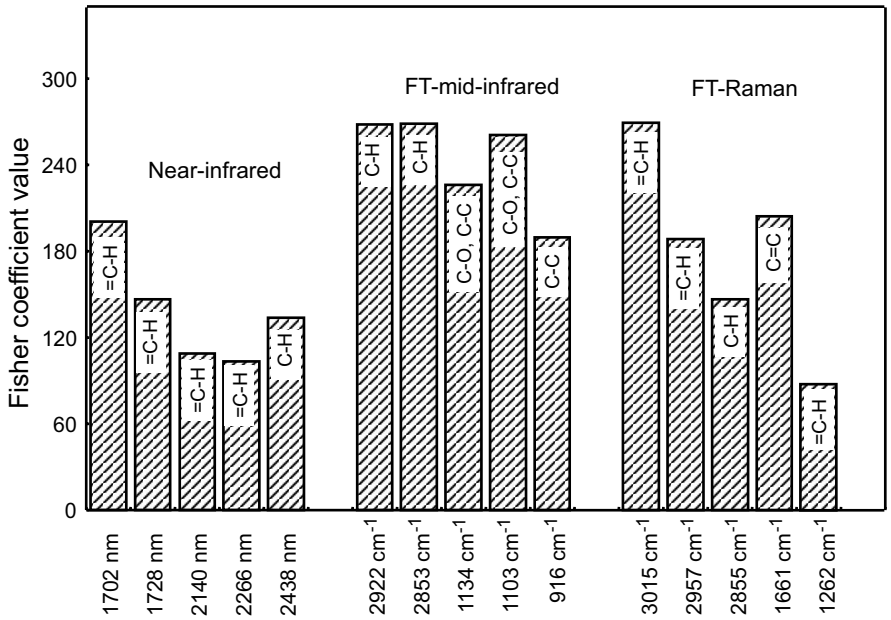

Fig. 10.21 The five most discriminant wavelengths (or wavenumbers) resulting from the study of near-infrared, FT-mid-infrared, and FT-Raman spectra of seven edible oil sources (corn, high oleic sunflower, peanut, rapeseed, soybean, sunflower, and virgin olive oils)

Some progress have been made in the development of new methods to detect adulteration, such as fraudulent mixtures of olive oil with hazelnut oil (Sayago et al. 2007), or to detect the oxidation degree of oils (Poulli et al. 2009a, b). The application of more advanced methods as EEFS and SFS makes the interpretation of the spectra more easy and informative than conventional spectroscopy.

Many fluorescent compounds present in virgin olive oil are involved in oxidation (e.g., phenols and vitamin E), and they evolve during different culinary practices such as frying. For that reason, fluorescence spectroscopy has recently been applied to evaluate the quality of thermoxidized oils (Tena et al. 2009, 2012). Other applications include the study of oil deterioration during long-term storage (Sikorska et al. 2008).

10.9 Conclusions

The previous sections have shown the potential of IR, Raman, and fluorescence spectroscopic techniques in oil analysis. NIR, MIR, and Raman spectra mainly contain information about unsaturated compounds. NIR spectroscopy can be used to determine the total level of unsaturation and the content of *cis* isomers. Excitation and

emission fluorescence spectra provide information about the minor compounds present in olive oil. The low cost and the possibility of coupling the NIR spectrometer to classical optical fibers provide a designed technique for implementation in continuous processes. MIR spectroscopy is classically used to determine the content of *trans* isomers, while information about *cis* isomers exists but is more limited. A MIR spectrometer seems to be an appropriate instrument for analytical laboratories. In fact, recent studies have demonstrated the great potential of MIR spectroscopy in the determination of classic chemical values and oil indices. The potential of this technique in the monitoring of oxidative processes is an additional advantage.

New developments in the instrumentation of Raman spectroscopy have promoted its importance for oil analysis. Raman spectra mainly contain information about *cis* and *trans* isomers. Due to the chemical origin of the bands, the information contained in the spectrum may be used to develop techniques for the determination of the total content of unsaturation, the type of unsaturation, and *cis/trans* isomer composition. In addition, a Raman spectrometer does not need a special sample-handling accessory and may be coupled to low-cost optical fibers.

In addition to the possibilities offered in quantitative analysis and in monitoring oxidative processes, IR and Raman spectroscopy show interesting perspectives in the characterization and adulteration detection of virgin olive oil. To compare the potential of NIR, MIR, and Raman spectroscopy in this domain, the spectra of 64 edible oils from seven varieties (corn, soybean, rapeseed, peanut, sunflower, high oleic sunflower, and virgin olive oils) were collected (Aparicio and Baeten 1998). The Fisher coefficient was used to underline the wavelengths and the wavenumbers having the highest power of varietal discrimination. Figure 10.21 displays, for each technique studied, the five most discriminant wavelengths or wavenumbers. NIR spectral data present Fisher coefficients lower than the data obtained in MIR and Raman spectroscopy. Four wavelengths underlined in NIR spectroscopy correspond to the C-H vibration of unsaturated groups. On the other hand, the wavenumbers extracted in MIR spectroscopy are characteristic of the C-H and C-C vibrations of the carbon skeleton and of the C-O of the ester groups. As in NIR spectroscopy, part of the Raman spectral data selected corresponds to the C-H vibration of unsaturated groups. The other wavenumbers are characteristics of C-H and C=C vibrations. Figure 10.10 clearly shows complementarity between vibrational spectroscopy (i.e., NIR and MIR spectroscopic techniques). This information can benefit from fluorescence spectroscopy, particularly in oxidation studies. Fluorescence spectroscopy is very versatile because it makes spectra acquisition possible in different modes (EEFS, SFS). These different modes provide several alternatives for a better interpretation of the spectra collected with conventional fluorescence spectroscopy to establish definitive and nonspeculative chemical assignments of the spectral bands like those in MIR, NIR, and Raman spectra.

References

Abbas O, Fernández Pierna JA, Codony R, von Holst C, Baeten V (2009) Assessment of the discrimination of animal fat by FT-Raman spectroscopy. J Mol Struct 924–926:294–300

Afran A, Newbery JE (1991) Analysis of the degree of unsaturation in edible oils by Fourier transforminfrared/attenuated total reflectance spectroscopy. Spectrosc-Int J 3:39–42

Ahro M, Hakala M, Kauppinen J, Kallio H (2002) Headspace FT-IR analysis of rapeseed oil oxidation. Appl Spectrosc 56:217–222

American Oil Chemists Society (AOCS) (1988) Officials methods and recommended practices of the American Oil Chemist's Society, method Cd 14–61. AOCS Press, Champaign

Aparicio R, Baeten V (1997) Possibilities offered by infrared and Raman spectroscopic techniques in virgin olive oil authentication. Olivae 69:38–43

Aparicio R, Baeten V (1998) Authentication of olive oil by FT-Raman. OCL 5:14–16

Aparicio R, Morales MT (1995) Sensory wheels: a statistical technique for comparing QDA panels – application to virgin olive oil. J Sci Food Agric 67:247–257

Aparicio R, Montaño J, Rodriguez-Izquierdo G (1977) Reactive power meter for nonsinusoidal systems. IEEE Trans Instru Meas 26:258–260

Aparicio R, Gutiérrez F, Rodríguez-Morales J (1992) Relationship between flavour descriptors and overall grading of analytical panels for virgin olive oil. J Sci Food Agric 58:555–562

Arnold RG, Hartung TE (1971) Infrared spectroscopy determination of degree of unsaturation of fats and oils. J Food Sci 36:166–168

Baeten V, Meurens M, Morales MT, Aparicio R (1996) Detection of virgin olive oil adulteration by Fourier transform Raman spectroscopy. J Agric Food Chem 44:2225–2230

Baeten V, Hourant P, Morales MT, Aparicio R (1998) Oil and fat classification by FT-Raman spectroscopy. J Agric Food Chem 46:2638–2646

Baeten V, Dardenne P, Aparicio R (2001) Interpretation of Fourier transform Raman spectra of the unsaponifiable matter in a selection of edible oils. J Agric Food Chem 49:5098–5107

Baeten V, Fernández Pierna JA, Dardenne P, Meurens M, García González DL et al (2005) Detection of the presence of hazelnut oil in olive oil by FT-raman and FT-MIR spectroscopy. J Agric Food Chem 53:6201–6206

Bailey GF, Horvat RJ (1972) Raman spectroscopic analysis of the cisltrans isomer composition of edible vegetable oils. J Am Oil Chem Soc 49:494–498

Banwell CN (1994) Fundamentals of molecular spectroscopy. McGraw-Hill, London

Baranska H, Labudzinska A, Terpinski J (1987) Laser Raman spectrometry: analytical applications. Ellis Horwood, Chichester

Barrow GM (1973) Physical chemistry. McGraw-Hill, New York

Bellon-Maurel V, Vigneau JL, Sévila F (1994) Infrared and near-infrared technology for the food industry and agricultural uses: on-line applications. Food Control 5:21–27

Belousov AI, Verzakov SA, von Frese JJ (2002) Applicational aspects of support vector machines. J Chemometr 16:482–489

Belton PS, Wilson RH, Sadeghi-Jorabchi H, Peers KE (1988) A rapid method for the determination of isolated trans double bonds in oils and fats using Fourier transform infrared spectroscopy combined with attenuated total reflectance. Lebensm Wiss Technol 21:153–157

Ben-Gal I (2005) Outlier detection. In: Maimon O, Rockach L (eds) Data mining and knowledge discovery handbook: a complete guide for practitioners and researchers. Kluwer Academic Publishers, New York, pp 131–146

Bernard JL, Sims LG (1980) IR spectroscopy for determination of total unsaturation. Res Dev 8:81–83

Blanco M, Villarroya I (2002) NIR spectroscopy: a rapid-response analytical tool. Trends Anal Chem 21:240–250

Burges CJC (1998) A tutorial on support vector machines for pattern recognition. Data Min Knowl Disc 2:121–167

Cayuela JA, Pérez Camino MC (2010) Prediction of quality of intact olives by near infrared spectroscopy. Eur J Lipid Sci Technol 112:1209–1217
Cayuela JA, García JM, Caliani N (2009) Predicción NIR de la humedad del fruto, acidez libre y contenido de aceite en aceitunas intactas. Grasas Aceites 60:194–202
Chapman D (1965) Infrared spectroscopy of lipids. J Am Oil Chem Soc 42:353–371
Chase B (1987) Fourier transform Raman spectroscopy. Anal Chem 59:881A–889A
Cook RD, Weisberg S (1982) Residuals and influence in regression. Chapman and Hall, London
Cowe IA, McNicol JW, Cuthbertson DC (1985a) A designed experiment for the examination of techniques used in the analysis of near infrared spectra. Part 1. Analysis of spectral structure. Analyst 110:1227–1232
Cowe IA, McNicol JW, Cuthbertson DC (1985b) A designed experiment for the examination of techniques used in the analysis of near infrared spectra. Part 2. Derivation and testing of regression models. Analyst 110:1233–1240
Defernez M, Kemsley K (1996) Potential pitfalls of chemometrics solutions to food authentication problems. In: Proceedings of food authenticity '96: Method for the measurement of food authenticity and adulteration. Institute of Food Research, Norwich
De Maesschalck R, Estienne F, Verdú-Andrés J, Candolfi A, Centner V et al (1999) The development of calibration models for spectroscopic data using principal component analysis. Internet J Chem 2:19
De Maesschalck R, Jouan-Rimbaud D, Massart DL (2000) The Mahalanobis distance. Chemometr Intell Lab 50:1–18
Despagne F, Massart DL (1998) Neural networks in multivariate calibration. Analyst 123:157R–178R
Diem M (1993) Introduction to modern vibrational spectroscopy. Wiley, New York
Dubois J, van de Voort FR, Sedman J, Ismail AA, Ramaswamy HR (1996) Quantitative Fourier transform infrared analysis for anisidine value and aldehydes in thermally stressed oils. J Am Oil Chem Soc 73:787–794
Dupuy N, Le Dréau Y, Ollivier D, Artaud J, Pinatel C, Kister J (2005) Origin of french virgin olive oil registered designation of origins predicted by chemometric analysis of synchronous excitation-emission fluorescence spectra. J Agric Food Chem 53:9361–9368
Egan WJ, Morgan SL (1998) Outlier detection in multivariate analytical chemical data. Anal Chem 70:2372–2379
Faber NM (2000) Response to comments on construction of confidence intervals in connection with partial least squares. J Chemometr 14:363–369
Faber NM, Bro R (2002) Standard error of prediction for multiway PLS – 1. Background and a simulation study. Chemometr Intell Lab 61:133–149
Fayolle PH, Picque D, Corrieu G (2000) On-line monitoring of fermentation processes by a new remote dispersive middle-infrared spectrometer. Food Control 11:291–296
Fenton AJ, Crisler RO (1959) Determination of cis unsaturation in oils by near-infrared spectroscopy. J Am Oil Chem Soc 36:620–623
Fernández Pierna JA, Wahl F, de Noord OE, Massart DL (2002) Methods for outlier detection in prediction. Chemometr Intell Lab 63:27–39
Fernández Pierna JA, Jin L, Wahl F, Faber NM, Massart DL (2003) Estimation of partial least squares regression (PLSR) prediction uncertainty when the reference values carry a sizeable measurement error. Chemometr Intell Lab 65:281–291
Fernández Pierna JA, Baeten V, Michotte Renier A, Cogdill RP, Dardenne P (2004) Combination of support vector machines (SVM) and near infrared (NIR) imaging spectroscopy for the detection of meat and bone meat (MBM) in compound feeds. J Chemometr 18:341–349
Fletcher R, Reeves M (1964) Function minimization by conjugate gradients. Comput J 7: 149–154
Galano T, Durán I, Correa CA, Roldán B, Rodriguez MI (2003) Simultaneous fluorometric determination of chlorophylls a and b and pheophytins a and b in olive oil by partial least squares calibration. J Agric Food Chem 51:6934–6940

Galeano T, Durán I, Correa CA, Roldán B, Rodriguez MI (2003) Simultaneous fluorometric determination of chlorophylls a and b and pheophytins a and b in olive oil by partial least squares calibration. J Agric Food Chem 51:6934–6940

Gallardo-González L, Osorio-Bueno E, Sánchez-Casas J (2005) Application of near infrared spectroscopy (NIRS) for the real-time determination of moisture and fat contents in olive pastes and wastes of oil extraction. Alimentación, Equipos y Tecnología 24:85–89

García-Gonzalez DL, van de Voort FR (2009) A novel wire mesh "cell" for studying lipid oxidative processes by fourier transform infrared spectroscopy. Appl Spectrosc 63:518–527

Gerrard DL, Birnie J (1992) Raman spectroscopy. Anal Chem 64:502R–513R

Geurts MD, Rinne HJ, Lawrence SH (1990) Alternative methods od dealing with outliers in forecasting sales with regression-based methods. In: Lawrence KD, Arthur JL (eds) Robust regression: analysis and application. Marcel Dekker, New York, pp 225–239

Giungato P, Aveni M, Rana R, Notarnicola L (2004) Modifications induced by extra virgin olive oil frying processes. Ind Aliment-Italy 43:369–375

Goddu RF (1957) Determination of unsaturation by near-infrared spectrophotometry. Anal Chem 29:1790–1794

Gonzaga FB, Pasquini C (2006) A new method for determination of the oxidative stability of edible oils at frying temperatures using near infrared emission spectroscopy. Anal Chim Acta 570:129–135

Grasseli JG, Bulkin BJ (1991) Analytical Raman spectroscopy. Wiley, New York

Guillén MD, Cabo N (1997) Infrared spectroscopy in the study of edible oils and fats. J Sci Food Agric 75:1–11

Guimet F, Ferré J, Boqué R, Rius FX (2004) Application of unfold principal component analysis and parallel factor analysis to the exploratory analysis of olive oils by means of excitation-emission matrix fluorescence spectroscopy. Anal Chim Acta 515:75–85

Harrick N (1967) Internal reflection spectroscopy. Wiley, New York

Hendra PJ (1997) Fourier transform Raman spectroscopy in pharmaceutical analysis and research. Int Lab 5:13A–13I

Hermoso M, Uceda M, García-Ortiz A, Jiménez A, Beltrán G (1999) Preliminary results of NIR "on line" measure of oil content and humidity in olive cakes from the two phases decanter. Acta Horticulturae 474:717–719

Herzberg G (1945) Molecular spectra and molecular structure. II. Infrared and Raman spectra of polyatomic molecules. Van Nostrand Reinhold, New York

Hirschfeld T, Chase B (1986) FT-Raman spectroscopy: development and justification. Appl Spectrosc 3:133–141

Holman RT, Edmondson PR (1956) Near infrared spectra of fatty acids and some related substances. Anal Chem 28:1533–1538

Hooke R, Jeeves FA (1961) Direct search solution of numerical and statistical problems. J Assoc Comput Mach 8:212–229

Hourant P (1995) Contrôle de qualité des matières grasses alimentaires par spectroscopie infrarouge. Catholic University of Louvain (UCL), Louvain-la-Neuve

Hourant P, Baeten V, Morales MT, Meurens M, Aparicio R (2000) Oil and fat classification by selected bands of near-infrared spectroscopy. Appl Spectrosc 54:1168–1174

Høy M, Steen K, Martens H (1998) Review of partial least squares regression prediction error in Unscrambler. Chemometr Intell Lab 44:123–133

Huang H, Yu H, Xu H, Ying Y (2008) Near infrared spectroscopy for on/in-line monitoring of quality in foods and beverages: a review. J Food Eng 87:303–313

International Union Pure and Applied Chemistry (IUPAC) (1992) Determination of content of isolated *trans*-unsaturated compounds by infrared spectrophotometry. In: Dieffenbacher A, Pocklington WD (eds) Standards methods for the analysis of oils, fats and derivatives, 7th edn. Blackwell Scientific Publication, Oxford, pp 99–102, Method 2.207

Ismail AA, van de Voort FR, Emo G, Sedman J (1993) Rapid quantitative determination of free fatty acids in fats and oils by Fourier transform infrared spectroscopy. J Am Oil Chem Soc 70:335–341

Ismail AA, Cocciardi RA, Alvarez P, Sedman J (2006) Infrared and Raman spectroscopy in food science. In: Hui YH (ed) Handbook of food science, technology and engineering. CRC Press, Boca Raton, pp 44.1–44.19

Jiménez-Márquez A, Molina-Díaz A, Pascual-Reguera MI (2005) Using optical NIR sensor for on-line virgin olive oils characterization. Sensors Actuat B 107:64–68

Jouan-Rimbaud D, Bouveresse E, Massart DL, de Noord OE (1999) Detection of prediction outliers and inliers in multivariate calibration. Anal Chim Acta 388:283–301

Keller S, Löchte T, Dippel B, Schrader B (1993) Quality control of food with near-infrared excited Raman spectroscopy. Fresenius J Anal Chem 346:863–867

Kennard RW, Stone LA (1969) Computer aided design of experiments. Technometrics 11:137–148

Kondepati VR, Heise HM (2008) The potential of mid- and near-infrared spectroscopy for reliable monitoring of bioprocesses. Curr Trends Biotechnol Pharm 2:117–132

Kuligowski J, Quintás G, de la Guardia M, Lendl B (2010) Analytical potential of mid-infrared detection in capillary electrophoresis and liquid chromatography: a review. Anal Chim Acta 679:31–42

Kyriakidis NB, Skarkalis P (2000) Fluorescence spectra measurement of olive oil and other vegetable oils. J AOAC Int 83:1435–1438

Lai YW, Kemsley EK, Wilson RH (1994) Potential of Fourier transform infrared spectroscopy for the authentication of vegetable oils. J Agric Food Chem 42:1154–1159

Lakowicz JR (1999) Principles of fluorescence spectroscopy, 2nd edn. Kluwer Academic Publishers, New York, pp 27–61

Lanser AC, Emken EA (1988) Comparison of FTIR and capillary gas chromatographic methods for quantitation of trans unsaturation in fatty acid methyl esters. J Am Oil Chem Soc 65:1483–1487

Lanser AC, List GR, Holloway RK, Mounts TL (1991) FTIR estimation of free fatty acid content in crude oils extracted from damaged soybeans. J Am Oil Chem Soc 68:448–449

Levin IW, Lewis EN (1990) Fourier transform Raman spectroscopy of biological materials. Anal Chem 62:1101A–1111A

Lewis EN, Kalasinsky VF, Levin IW (1988) Near-infrared Fourier transform Raman spectroscopy using fiber-optic assemblies. Anal Chem 60:2658–2661

Li Y, García-González DL, Yu X, van de Voort FR (2008) Determination of free fatty acids in edible oils with the use of a variable filter array IR spectrometer. J Am Oil Chem Soc 85:599–604

Li D, Sedman J, García-González DL, van De Voort FR (2009) Automated acid content determination in lubricants by FTIR spectroscopy as an alternative to acid number determination. J ASTM Int 6:1–12

Li-Chan ECY (1994) Developments in the detection of adulteration of olive oil. Trends Food Sci Technol 5:3–11

Li-Chan ECY (1996) The application of Raman spectroscopy in food science. Trends Food Sci Technol 7:361–370

Li-Chan ECY, Griffiths PR, Chalmers JM (2010a) Applications of vibrational spectroscopy in food science. Volume I: instrumentation and fundamental applications. Wiley, Chichester

Li-Chan ECY, Griffiths PR, Chalmers JM (2010b) Applications of vibrational spectroscopy in food science. Volume II: analysis of food, drink and related material. Wiley, Chichester

Ma K, van de Voort FR, Ismail AA, Sedman J (1998) Quantitative determination of hydroperoxides by FTIR spectroscopy using a disposable IR card. J Am Oil Chem Soc 75:1095–1101

Ma K, van de voort FR, Sedman J, Ismail AA (1999) *Trans* determination in fats and oils and margarine by FTIR spectroscopy using a disposable IR card. J Am Oil Chem Soc 76:1399–1404

Martens H, Naes T (1989) Multivariate calibration. Wiley, Chichester

Massart DL, Kaufman L (1983) The interpretation of analytical chemical data by the use of cluster analysis. Wiley Interscience, Chichester

Mossoba MM, Yurawecz MP, McDonald RE (1996) Rapid determination of the total *trans* content of neat hydrogenated oils by attenuated total reflection spectroscopy. J Am Oil Chem Soc 73:1003–1009

Muniategui S, Paseiro P, Simal J (1992) Medida del grado de insaturación de aceites y grasas comestibles por espectroscopia infrarroja y su relación con el índice de yodo. Grasas Aceites 43:1–5

Naes T, Isaksson T (1989) Selection of samples for calibration in near-infrared spectroscopy. Part I: general principles illustrated by example. Appl Spectrosc 43:328–335

Nicoletti GM (1990) La fluorescenza degli oli di oliva. Riv Ital Sost Grasse 67:389–396

O'Neill R (1971) Function minimization using a simplex procedure. Appl Stat-J Roy St 3:79–88

Osborne BG, Fearn T, Hindle PH (1993) Spectroscopy with application in food and beverage analysis. Longman Sci & Tech, Singapore, pp 1–77 and pp 120–141

Ozaki Y, Cho R, Ikegaya K, Muraishi S, Kawauchi K (1992) Potential of near-infrared Fourier transform Raman spectroscopy in food analysis. Appl Spectrosc 46:1503–1507

Panford JA, deMan JM (1990) Determination of oil content of seeds by NIR: influence of fatty acid composition on wavelength selection. J Am Oil Chem Soc 67:473–482

Patra D, Mishra AK (2002) Recent developments in multi-component synchronous fluorescence scan analysis. Trac-Trends Anal Chem 21:787–798

Pell RJ (2000) Multiple outlier detection for multivariate calibration using robust statistical techniques. Chemometr Intell Lab 52:87–104

Pfaffenberger RC, Dielman TE (1990) A comparison of regression estimators when both multicollinearity and outliers are present. In: Lawrence KD, Arthur JL (eds) Robust regression: analysis and applications. Marcel Dekker, New York, pp 243–270

Poulli KI, Chantzos NV, Mousdis GA, Georgiou CA (2009a) Synchronous fluorescence spectroscopy: tool for monitoring thermally stressed edible oils. J Agric Food Chem 57:8194–8201

Poulli KI, Mousdis GA, Georgiou CA (2009b) Monitoring olive oil oxidation under thermal and UV stress through synchronous fluorescence spectroscopy and classical assays. Food Chem 117:499–503

Rabiner LR, Gold B (1975) Theory and application of digital signal processing. Prentice-Hall, Englewood Cliffs

Ratnayake WMN, Pelletier G (1996) Methyl esters from a partially hydrogenated vegetable oil is a better infrared external standar than methyl elaidate for the measurement of total trans content. J Am Oil Chem Soc 73:1165–1169

Sadeghi-Jorabchi H, Hendra PJ, Wilson RH, Belton PS (1990) Determination of the total unsaturation in oils and margarines by Fourier transform Raman spectroscopy. J Am Oil Chem Soc 67:483–486

Sadeghi-Jorabchi H, Wilson RH, Belton PS, Edwards-Webb JD, Coxon DT (1991) Quantitative analysis of oils and fats by Fourier transform Raman spectroscopy. Spectrochim Acta A 47:1449–1458

Sato T (1994) Near-infrared spectroscopic analysis of deterioration indices of soybeans for process control in *oil* milling plant. J Am Oil Chem Soc 71:293–298

Sato T, Kawano S, Iwamoto M (1991) Near-infrared spectral patterns of fatty acid analysis from fats and oils. J Am Oil Chem Soc 68:827–833

Savitsky A, Golay MJE (1964) Smoothing and differentiation of data by simplified least square procedures. Anal Chem 36:1627–1630

Sayago A, García-González DL, Morales MT, Aparicio R (2007) Detection of the presence of refined hazelnut oil in refined olive oil by fluorescence spectroscopy. J Agric Food Chem 55:2068–2071

Schrader B (1996) Raman spectroscopy in the near-infrared – a most capable method of vibrational spectroscopy. Fresenius J Anal Chem 355:233–239

Scotter CNG (1997) Non-destructive spectroscopic techniques for the measurement of food quality. Trends Food Sci Technol 8:285–292

Sharma A, Schulman SG (1999) Mesurement of fluorescence spectra. In: Introduction to fluorescence spectroscopy. Wiley, New York, pp 69–99

Sikorska E, Romaniuk A, Khmelinskii IV, Herance R, Bourdelande JL, Sokorski M, Koziol J (2004) Characterization of edible oils using total luminescence spectroscopy. J Fluoresc 14:25–35

Sikorska E, Górecki T, Khmelinskii IV, Sokorski M, Koziol J (2005) Classification of edible oils using synchronous scanning fluorescence spectroscopy. Food Chem 89:217–225

Sikorska E, Khmelinskii IV, Sikorski M, Caponio F, Bilancia MT, Pasqualone A, Gomes T (2008) Fluorescence spectroscopy in monitoring of extra virgin olive oil during storage. Int J Food Sci Technol 43:52–61

Sinclair RG, McKay AF, Myers GS, Jones RN (1952) The infrared absorption spectra of saturated fatty acids and esters. J Am Oil Chem Soc 74:2578–2585

Skoog DA, West DM, Holler FJ (1992) Fundamentals of analytical chemistry. Saunders College Publ Int Edition, New York

Sleeter RT, Matlock MG (1989) Automated quantitative analysis of isolated (nonconjugated) *trans* isomers using Fourier transform infrared spectroscopy incorporating improvements in the procedure. J Am Oil Chem Soc 66:121–127

Snee RD (1977) Validation of regression models, methods and examples. Technometrics 19:415–428

Socrates G (1994) Infrared characteristic group frequencies: tables and charts. Wiley, New York

Stefanov I, Baeten V, Abbas O, Colman E, Vlaeminck B, De Baets B, Fievez V (2010) Analysis of milk odd- and branched-chain fatty acids using Fourier transform (FT)-Raman spectroscopy. J Agric Food Chem 58:10804–10811

Strasburg GM, Ludescher RD (1995) Theory and applications of fluorescence spectroscopy in food research. Trends Food Sci Technol 6:69–75

Tabachnick BG, Fidell LS (1983) Using multivariate statistics. Harper & Row, New York

Tai C, Gu X, Zou H, Guo Q (2002) A new simple and sensitive fluorometric method for the determination of hydroxyl radical and its application. Talanta 58:661–667

Tena N, García-González DL, Aparicio R (2009) Evaluation of virgin olive oil thermal deterioration by fluorescence spectroscopy. J Agric Food Chem 57:10505–10511

Tena N, Aparicio R, García-González DL (2012) Chemical changes of thermoxidized virgin olive oil determined by excitation-emission fluorescence spectroscopy (EEFS). Food Res Int 45:103–108

Ulberth F, Haider HJ (1992) Determination of low level *trans* unsaturation in fats by Fourier transform infrared spectroscopy. J Food Sci 57:1444–1447

Valeur B (2002) Molecular fluorescence: principles and applications. Wiley-VCH Verlag, Weinheim

van de Voort FR (1994) FTIR spectroscopy in edible oil analysis. Inform 5:1038–1042

van de Voort FR, Ismail AA (1991) Proximate analysis of foods by mid-FTIR spectroscopy. Trends Food Sci Technol 2:13–17

van de Voort FR, Sedman J, Emo G, Ismail AA (1992) Rapid and direct iodine value and saponification number determination of fats and oils by attenuated total reflectance/fourier transform infrared spectroscopy. J Am Oil Chem Soc 69:1118–1123

van de Voort FR, Ismail AA, Sedman J, Dubois J, Nicodemo T (1994a) The determination of peroxide value by Fourier transform infrared spectroscopy. J Am Oil Chem Soc 71:921–926

van de Voort FR, Ismail AA, Sedman J, Emo G (1994b) Monitoring the oxidation of edible oils by Fourier transform infrared spectroscopy. J Am Oil Chem Soc 71:243–253

van de Voort FR, Ismail AA, Sedman J (1995) A rapid automated method for the determination of cis and trans content of fats and oils by Fourier transform infrared spectroscopy. J Am Oil Chem Soc 72:873–880

van de Voort FR, Memon KP, Sedman J, Ismail AA (1996) Determination of solid fat index by FTIR spectroscopy. J Am Oil Chem Soc 73:411–416

van de Voort FR, Cocciardi R, Sedman J, Juneau S (2007a) An automated FTIR method for the routine quantitative determination of moisture in lubricants. Talanta 72:289–295